On heart failure mechanics and hemodynamics

Pola, Karin

2025

Document Version:
Publisher's PDF, also known as Version of record

On heart failure mechanics and hemodynamics

KARIN POLA
DEPARTMENT OF CLINICAL PHYSIOLOGY | FACULTY OF MEDICINE | LUND UNIVERSITY

On heart failure mechanics and hemodynamics

On heart failure mechanics and hemodynamics

Karin Pola

LUND
UNIVERSITY

Thesis for the degree of Doctor of Philosophy in Medicine
Thesis advisors: Prof. Håkan Arheden and Dr. Per Arvidsson
Faculty opponent: Dr. Patricia Bandettini

To be presented for public critique in Föreläsningssal 3, Blocket, Skånes universitetssjukhus, Lund
on Friday June 13th 2025 at 09:15.

Organization: LUND UNIVERSITY **Date of issue:** June 13th 2025

Author: Karin Pola

Title: On heart failure mechanics and hemodynamics

Abstract:

Heart failure is a common condition with a high burden of morbidity and mortality globally. Despite modern advancements in diagnostic evaluation and therapeutic strategies, challenges remain in providing optimal treatment for the individual patient. Heart-failure phenotyping requires imaging modalities for assessment of structures and function. This thesis is based on four studies which apply novel, in-house developed methods on cardiovascular magnetic resonance (CMR) imaging for evaluation of heart function and intraventricular blood flow.

The aim was to investigate if these novel methods can improve our understanding of heart dysfunction in patients at risk for or with established heart failure, and assess the potential use as future diagnostic instruments in clinical practice. The main methods were non-invasive pressure-volume loops, and 4D-flow CMR for analysis of intraventricular kinetic energy and hemodynamic forces of the blood.

The results in Study I show that non-invasive pressure-volume loops detect different responses to altered preload and afterload in patients with hypertrophic cardiomyopathy compared to in healthy participants. Study II demonstrates that in patients with precapillary pulmonary hypertension, the right ventricle acts more like a pressure pump than a volume pump, as opposed to in healthy controls. The data in Study III indicate that 4D-flow CMR may detect hemodynamic abnormalities in patients with hypertrophic cardiomyopathy, even when echocardiographic flow measurements are normal. Finally, the data in Study IV suggest that 4D flow CMR may be of value in clinical evaluation of patients with heart failure and left bundle branch block where cardiac resynchronization therapy is considered.

In conclusion, novel biomarkers on CMR provide new insights in the pathophysiology of various phenotypes of heart failure, and may be of clinical value complementary to more established measures of heart dysfunction.

Key words: Heart failure, magnetic resonance imaging, 4D flow, pressure-volume loops, hypertrophic cardiomyopathy, pulmonary hypertension, cardiac resynchronization therapy

Language: English **Number of pages:** 120

ISSN: 1652-8220

ISBN: 978-91-8021-725-5

Signature_____ Lund 2024-04-29

On heart failure mechanics and hemodynamics

Karin Pola

LUND
UNIVERSITY

Faculty Opponent

Dr. Patricia Bandettini
National Institutes of Health
Washington D.C., USA

Evaluation Committee

Prof. Petter Dyverfeldt
Linköping University
Linköping, Sweden

Dr. Karin Tran Lundmark
Lund University
Lund, Sweden

Dr. Patrik Sundblad
Karolinska Institutet
Stockholm, Sweden

Cover: Nora Nordin, 2025

Faculty of Medicine, Department of Clinical Physiology, Lund Cardiac MR Group
ISBN: 978-91-8021-725-5
ISSN: 1652-8220
Lund University, Faculty of Medicine Doctoral Dissertation Series 2025:72
Printed in Sweden by Media-Tryck, Lund University, Lund 2025

What stands in the way becomes the way.

— Marcus Aurelius

Contents

List of papers

1 **Non-invasive pressure-volume loop analysis in left ventricular load manipulation**

K. Pola, C.B. Kristensen, W.D. Watson, P.G. Green, B. Raman, S. Neubauer, O.J. Rider, C. Hassager, R. Møgelvang, H. Arheden, P.M. Arvidsson
Manuscript

2 **Increased biventricular hemodynamic forces in precapillary pulmonary hypertension**

K. Pola, E. Bergström, J. Töger, G. Rådegran, P.M. Arvidsson, M. Carlsson, H. Arheden, E. Ostenfeld
Scientific Reports, 12:19933 (2022)

3 **Flow inefficiencies in non-obstructive HCM revealed by kinetic energy and hemodynamic forces on 4D flow CMR**

K. Pola, Z. Ashkir, S. Myerson, H. Arheden, H. Watkins, S. Neubauer, P.M. Arvidsson, B. Raman
European Heart Journal - Imaging Methods and Practice, 2:3 (2024)

4 **Hemodynamic forces from 4D flow magnetic resonance imaging predict left ventricular remodeling following cardiac resynchronization therapy**

K. Pola, A. Roijer, R. Borgquist, E. Ostenfeld, M. Carlsson, Z. Bakos, H. Arheden, P.M. Arvidsson
Journal of Cardiovascular Magnetic Resonance, 25:45 (2023)

Popular science summary

Heart failure is a condition with decreased heart function, where the blood circulation is not able to deliver sufficient oxygen and nutrition to the body. Despite modern advancements in treatment strategies, heart failure remains one of the leading causes of death worldwide. Heart failure is not *one* disease, instead there can be several underlying causes behind the reduced heart function, and patients can present with a wide range of symptoms. New methods for evaluating heart function are therefore needed to improve our understanding of heart dysfunction and provide better healthcare for the individual patient.

This thesis is based on four studies which apply novel magnetic resonance imaging methods for evaluation of heart function and blood flow within the heart. The purpose was to investigate if these novel methods can improve our understanding and diagnostics of heart dysfunction.

Three main methods were used to study the relation between pressure and volume of the heart, the energy of the blood due to its motion, and the forces between the blood within the heart and the surrounding heart muscle.

The results provide new insights in heart dysfunction, showing abnormal pumping and blood-flow patterns of the hearts in patients. Moreover, the results indicate that these novel methods may be of value in clinical evaluation of patients with heart failure, complementary to more established measures. Better understanding of heart dysfunction is the foundation for the development of new treatments that can improve the prognosis and quality of life for the individual patient.

Populärvetenskaplig sammanfattning

Hjärtsvikt innebär att hjärtats pumpförmåga är nedsatt och att blodcirkulationen inte kan tillgodose kroppens behov av syre och näring. Trots stora framsteg med moderna behandlingsmöjligheter är hjärtsvikt fortfarande en av de främsta dödsorsakerna globalt. Hjärtsvikt är inte en enskild sjukdom, utan det kan finnas flera bakomliggande orsaker till nedsatt hjärtfunktion. Dessutom kan patienter uppvisa många olika symptom. Därför är det viktigt att hitta bättre metoder för bedömning av hjärtfunktion, som kan leda till bättre förståelse för det sjuka hjärtat samt mer ändamålsenlig sjukvård för patienterna.

Denna avhandling baseras på fyra delarbeten där nya metoder med magnetkameraundersökning används för att utvärdera hjärtats funktion och blodflöde. Syftet var att undersöka om dessa nya metoder kan förbättra vår förståelse och diagnostik gällande hjärtsjukdomar.

De tre centrala metoderna i avhandlingen studerar relationer mellan tryck och volym inuti hjärtat, blodets rörelseenergi, och krafter mellan blodet inuti hjärtat och den omslutande hjärtmuskeln.

Resultaten bidrar till en utökad förståelse för avvikande pumpfunktion och blodflödesmönster hos patienter med hjärtsvikt. Dessutom tyder resultaten på att de nya metoderna kan vara värdefulla inom sjukvården för bedömning av patienter med hjärtsvikt, som komplement till mer etablerade undersökningsmetoder. Förbättrad förståelse för hjärtsvikt och de olika bakomliggande orsakerna är grundläggande för att kunna utveckla nya behandlingsmetoder som förbättrar den enskilda patientens prognos och livskvalitet.

Abbreviations

4D flow Four-dimensional flow

bSSFP balanced steady-state free precession

CMR Cardiovascular magnetic resonance imaging

CRT Cardiac resynchronization therapy

DCM Dilated cardiomyopathy

ECG Electrocardiogram

HCM Hypertrophic cardiomyopathy

HDF Hemodynamic forces

KE Kinetic energy

LBBB Left bundle branch block

PH$_{precap}$ Precapillary pulmonary hypertension

PV loop Pressure-volume loop

En volontärs betraktelser i magnetkameran

Magnetresonans
Resonerar med själen
Ger mig ett syfte

Ge mig ett syfte
Ropade jag till världen
Framför ögonen

Framför ögonen
Bara den gråa linjen
Centrerar min kropp

Centrerar min kropp
Dekonstruerar hjärtat
Synar alla slag

Alla slagen syns
Om jag ligger still under
Kamerans solon

Kamerans solon
Till heliumets basgång
Och tankens toner

Tankens toner och
Det så eviga bruset
Får gilla läget

Jag gillar läget
Gör allt för vetenskapen
Ställer alltid upp

Ställer alltid upp
Med mitt bultande hjärta
Mitt hjärta bultar

Mitt hjärta bultar
I takt och färg på en skärm
Så photogenique!

Så photogenique!
Säger forskningsledaren
Jag blir generad

Jag blir generad
Av alla komplimanger
Om mitt hjärtas slag

Och mitt hjärtas slag
Resonerar med själen
Magnetresonans

Nora Nordin, 2021

To Babi and Farmor,
Thank you for paving the way.

Part I

Research Context

Chapter 1

Background

1.1 The heart - structure and function

The function of the heart is to pump blood and serve the body with oxygen and nutrition. An overview of the anatomy of the heart is shown in Figure 1.1. There are four chambers in the heart, where the two ventricles constitute the main pumping instruments, and the two atria mainly act as reservoir and conduit systems in the healthy heart. The heartbeat can be divided into two main phases called systole and diastole. In systole, the ventricles contract and eject blood. The left side of the heart pumps blood towards the main circulation of the body, whereas the right side of the heart pumps towards the lung circulation. In diastole, the ventricles relax and are filled with blood to prepare for the next round of ventricular contraction. The left side of the heart is filled with well oxygenated blood coming from the lung circulation, whereas the right side of the heart is filled with less oxygenated blood coming from the main circulation of the body. The two circulations are thus separate systems, but connected serially via the heart.

Heart failure

In patients with heart failure, the heart function is impaired and the pumping capacity is, under normal pressure conditions, unable to meet the circulatory demand of oxygen and nutrients required for the metabolism. Chronic heart failure is a common condition where up to 50% of patients die within five years after diagnosis (1).

Impaired heart function can be caused by several pathological conditions, where

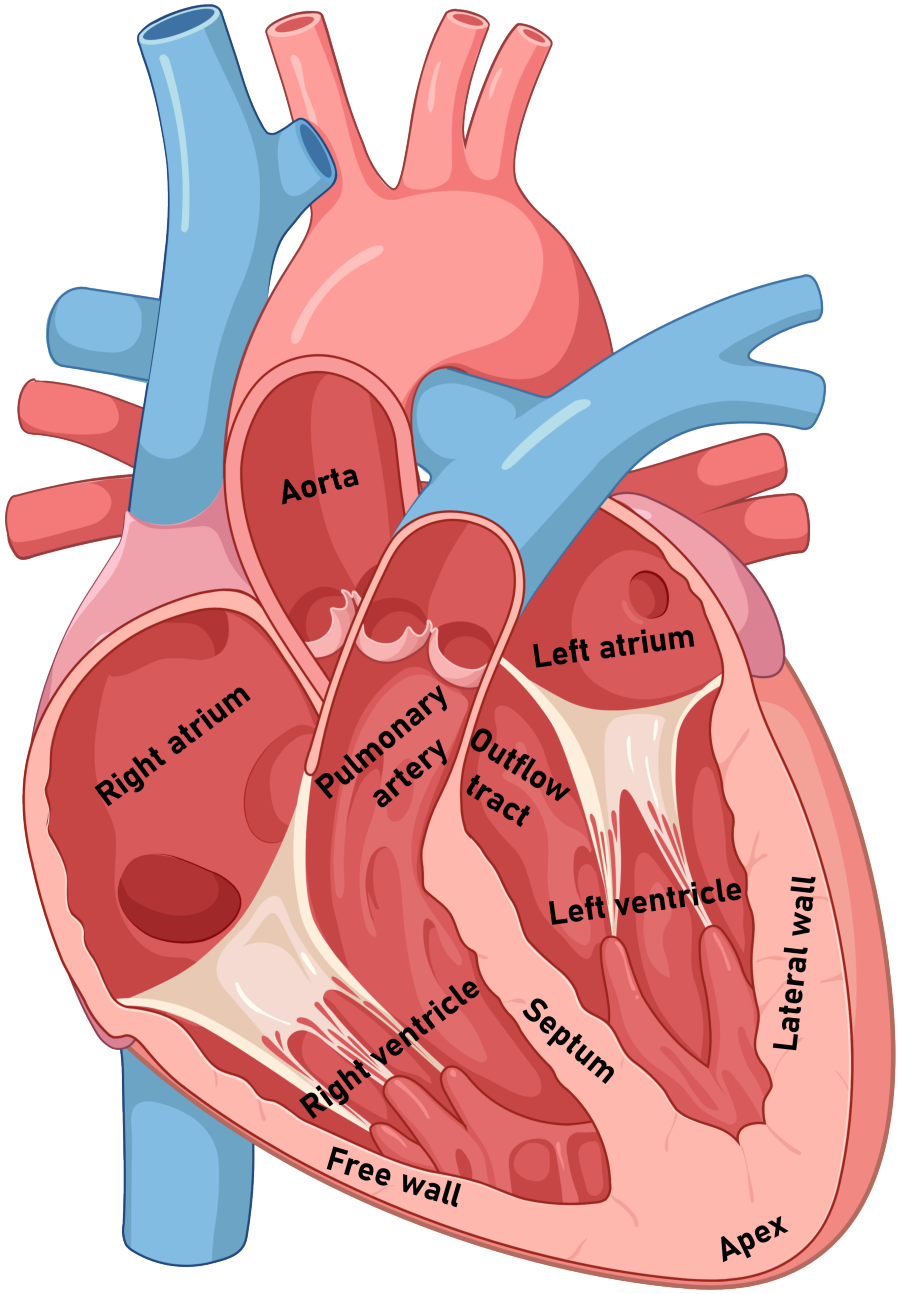

Figure 1.1: The human heart. Image created partly in BioRender. Pola, K. (2025) https://BioRender.com/h6243e9

structural or functional abnormalities result in inadequate blood volume pumped by the heart every minute, known as cardiac output. Commonly, the underlying pathologies behind heart failure affect primarily the left side of the heart. However, the right side of the heart can also be affected, either by primary pathologies or by failure secondary to left-sided failure.

The body can sometimes compensate for the reduced heart function, such as by increasing the heart rate and total blood volume in the circulatory system, which is induced by an up-regulation of the sympathetic nervous system and the release of cathecolamines. When the heart is filled with more blood, the heart muscle becomes more stretched, which leads to stronger contractions up to a certain limit, according to the Frank-Starling mechanism. With increased heart rate and total blood volume, the body may maintain sufficient cardiac output despite reduced pumping capacity of the heart.

With time, the heart may not be able to keep up with the increased heart rate and blood volume, which can lead to increasing pressures within the heart. When the heart works under these unfavorable conditions, the anatomy of the heart may remodel, leading to enlarged cavities of the heart or an abnormally thick heart muscle wall. The patient can experience symptoms of heart failure, which typically include shortness of breath, dry cough, ankle swelling or fatigue (2). Patients with heart failure can be classified according to the severity of symptoms, where the New York Heart Association (NYHA) has defined the following four functional stages (3):

I – No limitation of physical activity
II – Slight limitation of physical activity, but comfortable at rest
III – Marked limitation of physical activity, but comfortable at rest
IV – Severe limitation of physical activity, and symptoms at rest

This thesis studied patients at risk for, or with established chronic heart failure, due to various conditions affecting the left or right side of the heart. Study I examined alterations in the pressure-volume relations of the heart, Study II analyzed the blood flow within the hearts of patients with elevated pressure and resistance in the lung circulation, Study III evaluated patients with adverse thickening of the heart muscle, and Study IV investigated a new method for clinical evaluation of patients with disturbances in the electrical conduction system of the heart. The study populations in the four studies thus exhibited different variations of heart pathology, and were at different NYHA stages of symptom burden.

Chapter *1.1 The heart - structure and function* intends to provide an introduction to the normal physiology of the heart and circulatory system, followed by the principal mechanisms behind the various conditions of heart pathology in each of the four studies. The second part *1.2 Cardiovascular magnetic resonance* presents an overview of the physics behind cardiovascular magnetic resonance imaging, and the methods applied in this thesis for evaluation of heart failure mechanics and hemodynamics.

1.1.1 *Pressure-volume relations*

The blood circulation of the body is governed by flow, pressure and resistance. For blood to flow, enough pressure must be generated by the heart to overcome the resistance of the vessels. Blood flows from areas of higher pressure towards areas of lower pressure, following Ohm's law of an electric circuit applied to hemodynamics:

$$Flow = \frac{\Delta Pressure}{Resistance}$$

The relationship between pressure and volume during the heartbeat can be visualized in a Wiggers diagram (Figure 1.2), named after the physician Carl Wiggers (1883-1963) who developed this chart more than a century ago (4).

To eject blood in *systole*, the left ventricle needs to generate enough pressure to produce a positive pressure gradient from the left ventricle towards the connecting large blood vessel, called the aorta. Blood flows from the left ventricle towards the circulation of the body when the ventricle overcomes the *afterload*. Afterload refers to the resistance the heart works against to eject blood, and is proportional to the average pressure in the aorta. At the very beginning of systole, there is a phase called isovolumetric contraction, where the ventricle contracts with maintained volume and increases the pressure within the ventricle. During isovolumetric contraction, all valves are closed between the atria and ventricle and between the ventricle and the aorta. As shown in the Wiggers diagram, the absolute difference in pressure between the left ventricle and the aorta required for blood flow is relatively small compared to the global pressure in the ventricle.

In *diastole*, the ventricles are filled with blood and the muscle wall of the heart is stretched, resulting in a lengthening of the contractile elements similar to extending a spring. The degree of stretch of the ventricular muscle fibers prior to contraction is referred to as *preload*, and is largely determined by the blood volume returning to

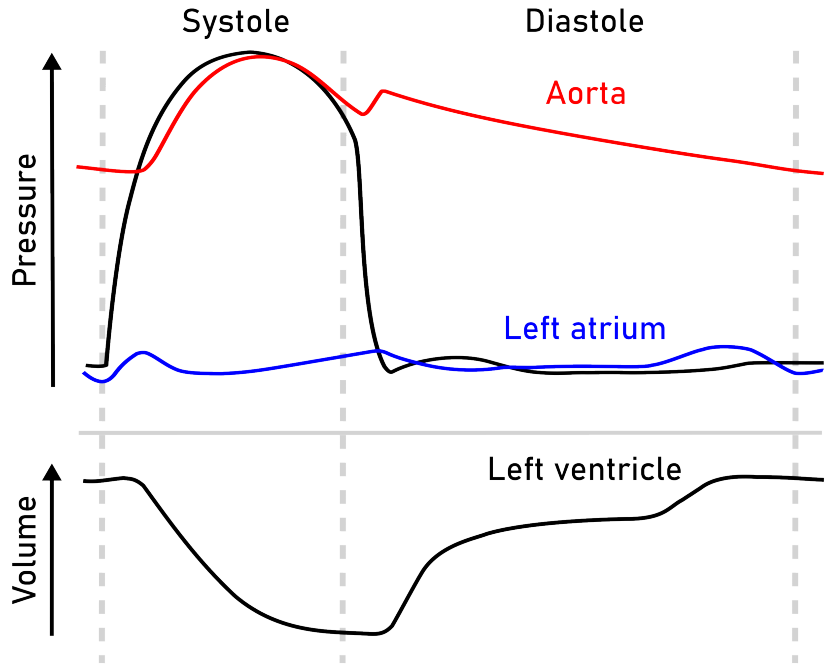

Figure 1.2: The relationship between pressure and volume in the left side of the heart during one heartbeat, visualized in a simplified Wiggers diagram.

the heart and the ventricular volume at the end of diastole. Ventricular relaxation entails both active and passive stretching of the muscle fibers. Active stretching requires energy to release the bonds between the muscle fibers, primarily by calcium pumps on the cellular level. Passive stretching does not require energy directly, but relies on the elastic recoil of the heart tissue when the myocardial fibers return to their resting state after contraction.

Diastole can be divided into three phases called early filling, diastasis and atrial contraction. In the healthy heart, early filling is the main contributor to ventricular filling. In the early filling phase, a pressure gradient is created with lower pressure in the ventricle than in the atrium, which results in a rapid blood flow towards the ventricle (5; 6). Should the ventricle not be able to relax properly, the resulting pressure gradient may be insufficient for optimal ventricular filling and the heart can be afflicted with diastolic dysfunction. Early diastolic filling is followed by the phase called *diastasis*, when the heart is in volumetric equilibrium and there is a pause in the blood flow despite open valves between the atrium and the ventricle (7). The duration of the diastasis is longer at lower heart rates, and when the heart

rate increases, the duration of the diastasis is gradually shortened (8). At heart rates of around 80 beats per minute, the diastasis disappears and the early and late phase of diastole merge. At the end of diastole, the atria contract and squeeze in the final blood volume and complete ventricular filling.

Pathologies in the heart and blood circulation can disrupt the physiological pressure-volume balance and impair ventricular contraction and relaxation, leading to dysfunctional pumping of the heart. Studying pressure-volume relations within the heart can provide insights into the mechanics and hemodynamics of the heart (9; 10). Pressure-volume relations within the heart have been measured invasively for decades to investigate physiological mechanisms in healthy and pathological conditions. A common way to study left ventricular pressure-volume relations is by creating a pressure-volume loop where time-resolved volumes and pressures are plotted in an xy-graph (Figure 1.3). Computation of left ventricular pressure-volume loops enable analysis of heart function, including ventricular efficiency and the amount of energy required for one heartbeat, which are associated with the oxygen consumption of the heart (11; 12).

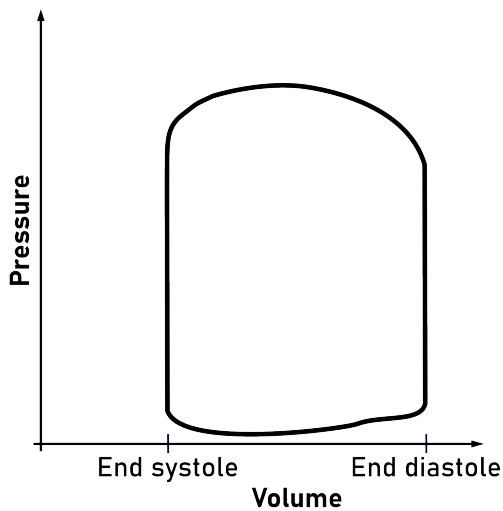

Figure 1.3: Pressure-volume loop of the left ventricle during one heartbeat, where the x-axis shows volumes and the y-axis shows pressures within the left ventricle.

In patients with heart failure, the pressure-volume relations during the heartbeat can be disturbed, resulting in abnormal pressure-volume loops. Previous studies with experimental models of manipulation of preload and afterload, have demon-

strated changes in the mechanics and hemodynamics of the heart on pressure-volume loops (13). Historically, calculation of pressure-volume loops have required invasive techniques with a catheter placed in the ventricle for measurements of pressures and volumes throughout the heartbeat. As with all invasive procedures, the method carries risks and discomfort for the patient. Moreover, although an invasive catheter is the gold standard method for pressure measurements within the heart, the volumes of the heart can be better measured with imaging modalities, such as cardiovascular magnetic resonance.

Recent technical developments have enabled non-invasive computation of pressure-volume loops, using volumetric assessment from cardiovascular magnetic resonance imaging, combined with non-invasive brachial blood-pressure measurements (described in more detail in Chapter 3.3) (14). This non-invasive tool has been tested against invasive measurements in experimental models with alterations in preload (14; 15) and in human (16). Furthermore, previous studies have demonstrated hemodynamic changes on non-invasive pressure-volume loops in various conditions affecting the heart, such as during pharmacological stimulation of the sympathetic nervous system with dobutamine in healthy controls (17) and in patients with right ventricular volume overload (18), in experimental myocardial infarction (19), and in children with closure of an atrial septal defect (20).

Patients with heart failure benefit from unloading, meaning reducing the work load of the heart regarding pressure and volume. Unloading the heart has been shown to improve the metabolic and energetic conditions of the heart, leading to increased pumping efficiency (21), and reducing symptoms and the risk for death (22). Assessing pressure-volume relations can thus be a valuable tool when evaluating patients with heart failure and their response to treatments, but the invasive nature of conventional procedures limits the clinical appliance. The purpose of Study I was therefore to assess the performance of non-invasive pressure-volume loops for analysis of heart function when manipulating ventricular preload and afterload in healthy participants and in patients with abnormal ventricular filling.

The right side of the heart

Contrary to the high-pressure system of the systemic circulation, the lung circulation operates under low pressures. Since the right ventricle pumps blood to the lung circulation where the resistance is low under normal conditions, the right ventricle is optimized to work with a relatively low afterload, and has a thin muscle wall

and works with low pressures within the ventricle. In conditions with increased resistance and thus higher blood pressure in the lung circulation, the right ventricle needs to overcome a greater afterload to eject blood.

Observations of elevated pressure and resistance in the lung circulation have been described since the late 1800's (23), and today the conditions are referred to as *pulmonary hypertension*. In patients with pulmonary hypertension, the right ventricle may remodel with pathological thickening of the heart muscle and eventually enlargement of the ventricular cavity (Figure 1.4), as the heart fails to compensate for the elevated pressures. The right-ventricular overload of pressure and volume can also lead to anatomical remodeling with septal bowing into the left ventricle. Pulmonary hypertension may lead to decreased cardiac output from the right ventricle and right-sided heart failure. Consequently, the filling of the left ventricle can be disturbed when the blood volume pumped from the right to the left side of the heart is reduced, resulting in decreased left ventricular preload.

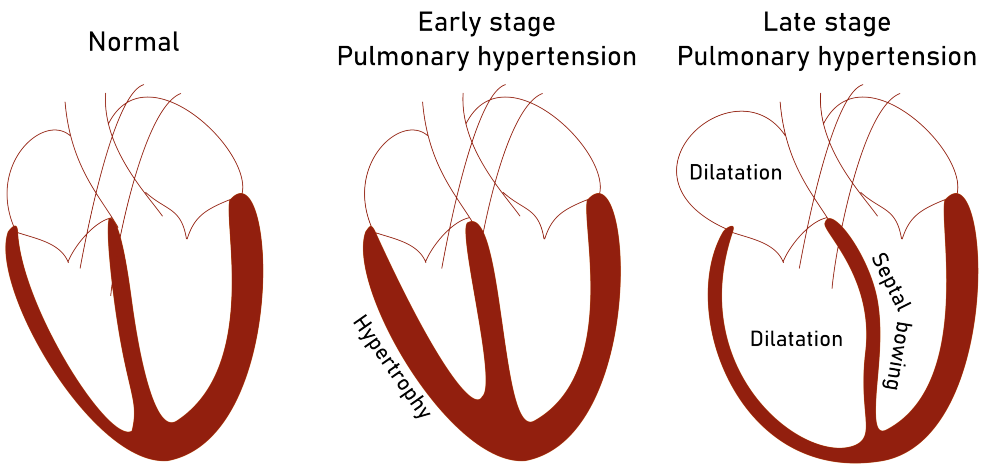

Figure 1.4: Visualization of the anatomy in pulmonary hypertension with remodeling of the heart in the early and late stages.

In patients with pulmonary hypertension, there is a chronic increase in the pressure and resistance of the blood vessels in the lung circulation. The underlying causes behind pulmonary hypertension are heterogenous, and patients can be classified into the following five main groups based on the characteristics of the condition (24):

I – Pulmonary arterial hypertension
II – Pulmonary hypertension associated with left heart disease
III – Pulmonary hypertension associated with lung disease
IV – Pulmonary hypertension with chronic obstruction in the pulmonary arteries
V – Pulmonary hypertension with unclear or multi-factorial mechanisms

Of these five groups, group II is the most common condition (25), since primary left-heart disease is more frequent than primary right-heart disease in the general population. With impaired left ventricular function, blood may accumulate in the lung circulation due to left-sided backward failure, resulting in increased right-ventricular afterload.

Groups I and IV are caused by pathology in the vessels of the lung circulation, and are classified as *precapillary pulmonary hypertension*. These conditions are predominately linked to right-sided heart failure, yet patients may also exhibit secondary left-sided heart failure. Groups I and IV are rare conditions with approximately 10-30 new cases in each group every year per million adults (26). Despite modern treatments, the survival rates remain low with a 5-year mortality of around 50 % in group I (27) and 30 % in group IV (28).

Initially, patients often develop precapillary pulmonary hypertension without any specific signs or symptoms (29), which is why a timely diagnosis and initiation of dedicated treatments can be challenging. Clinical evaluation of patients with precapillary pulmonary hypertension include invasive measurements of pressure and resistance in the heart and in the lung circulation, to make a correct diagnosis and to assess treatment effect over time. New, non-invasive methods for assessment of heart function are therefore warranted to better understand the pathophysiology in precapillary pulmonary hypertension, which may in the future improve clinical management of these patients. The purpose of Study II was to investigate if the heart function in patients with precapillary hypertension can be better understood by analysis of blood-flow patterns using novel methods on cardiovascular magnetic resonance imaging.

Cellular structures

Every day, the heart beats around 100 000 times in an adult, and every heartbeat is an energy-costly procedure. The heart is a smooth muscle composed of a thick

layer of myocardium embraced by an inner thin layer of endocardium lining the cavities, and an outer thin layer of epicardium. The myocardium consists of specialized cells called *myocytes*, and extracellular matrix components rich in collagen. Each myocyte contains contractile elements called sarcomeres, which consist of filaments of proteins called actin and myosin that participate in sliding motions during contraction and relaxation (30; 31). The high energy demand of the cells is met by a dense network of small blood vessels, called capillaries, and an abundance of mitochondria within each cell.

The micro anatomy of the heart is neatly organized to achieve energy-efficient pumping and generate blood flow. In the myocardium, the myocytes are arranged in sheets by connections through cell-cell junctions called intercalated disks. Thus, adjacent myocytes can function as one larger unit by mechanical and electrical connections. Furthermore, cellular cohesion is facilitated by collagen that anchors and aligns sheets of myocytes. To optimize the pumping of the ventricle, sheets of myocytes are oriented in a helix pattern allowing for a twisting motion of the ventricle during contraction and relaxation.

Pathology of the cellular structures of the heart can lead to dysfunctional contraction and relaxation. Over time, cellular pathologies may induce the development of heart failure. The most common inherited heart disease is called *hypertrophic cardiomyopathy*, which occurs in around 1 in 500 people in the general population (32) and frequently leads to heart failure. Hypertrophic cardiomyopathy is a condition with an exceedingly thick heart muscle, and has been described clinically since the late 1950's (33; 34). Not only are the myocytes enlarged and deformed in hypertrophic cardiomyopathy, the architecture of the micro anatomy is also disorganized (35), primarily affecting the left ventricular geometry and function. The extracellular matrix contains excessive amounts of fibrosis and an undermined network of blood vessels, contributing to stiffness and oxygen deficit of the heart muscle (36; 37; 38; 39). The myocytes may also suffer from reduced mechanical and energetic efficiency due to impaired mitochondrial function and disarray in the intracellular contractile elements (40).

Clinical diagnosis of hypertrophic cardiomyopathy is defined as a maximum wall thickness of ≥ 15 mm at end diastole, or ≥ 13 with a family history of hypertrophic cardiomyopathy (41). There are several know genes associated with hypertrophic cardiomyopathy, where the most common ones are MYH7 and MYBPC3 (42). According to current knowledge, genetic variants associated with hypertrophy can

be found in around 40-60% of patients with hypertrophic cardiomyopathy (43). However, not all patients with a positive genetic testing develop an abnormally thick heart muscle. Patients carrying genetic variants associated with hypertrophic cardiomyopathy but with a normal anatomy of the heart, can be described as *genotype positive* and *phenotype negative*. Contrarily, in numerous patients with hypertrophic cardiomyopathy, no pathogenic or likely pathogenic genetic variant can be identified, and these patients can be described as *genotype negative* and *phenotype positive*.

Hypertrophic cardiomyopathy can present with various patterns of remodeled left ventricular anatomy (Figure 1.5). The hypertrophy can be local, affecting only parts of the left ventricle, or global where the entire ventricle is somewhat evenly thickened. The pattern of left ventricular hypertrophy can be characterized using imaging modalities, such as echocardiography or cardiovascular magnetic resonance, and described as septal, reverse septal, mid-ventricular, apical, or concentric hypertrophy (44; 45; 46).

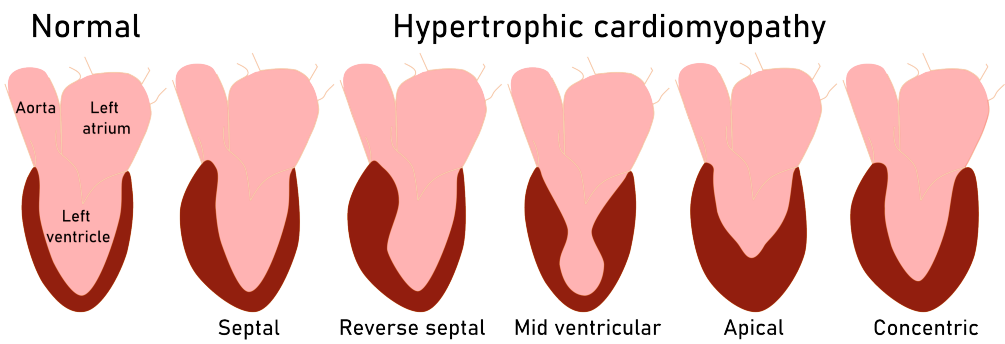

Figure 1.5: Schematic illustrations of a heart with normal ventricular anatomy, and hearts with hypertrophic cardiomyopathy and different patterns of left ventricular remodeling.

The thick muscle wall of the left ventricle in hypertrophic cardiomyopathy can affect the left ventricular outflow tract, connecting the ventricle with the aorta, and cause obstruction of the blood flow in systole. Approximately 70% of patients with hypertrophic cardiomyopathy suffer from left ventricular outlflow tract obstruction (47). In some patients, obstruction in the left ventricular outflow tract occurs only during exercise when the circulatory demand is increased, whereas in more severe cases, patients exhibit obstruction both during exercise and at rest. The primary mechanisms behind obstruction are hypertrophy in the basal part of the septum,

and systolic-anterior motion of the mitral valve leaflets due to anatomic alteration in the mitral valve apparatus. When the outflow tract is constringed, the resistance increases which leads to increasing pressures in the ventricle, which in turn may further exacerbate the global ventricular hypertrophy.

Clinically, left ventricular outflow tract obstruction is associated with an increased risk of heart failure and a poorer prognosis for the patient (48; 49). However, the vast majority of patients live asymptomatically for years before suddenly experiencing deterioration. Despite regular medical examinations, challenges remain regarding prognostication and risk stratification when standard diagnostic tools, such as ultrasound of the heart, report normal values. The purpose of Study III was therefore to investigate if novel methods for blood-flow analysis, using cardiovascular magnetic resonance imaging, can provide insights in the heart function of patients with hypertrophic cardiomyopathy, without left ventricular outflow tract obstruction and with normal blood-flow parameters measured with ultrasound of the heart.

Electrical conduction system

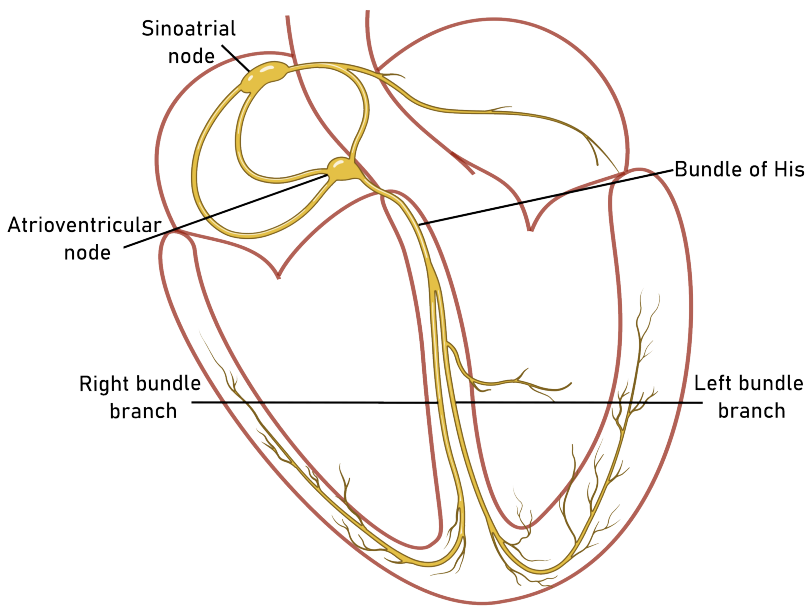

Figure 1.6: Overview of the electrical conduction system of the heart. Image created partly in BioRender. Pola, K. (2025) https://BioRender.com/uw39lzg

Muscular contraction of the heart is preceded by electrical excitation of the myocytes, and the heart operates as one electrical unit via cell-cell junctions. The conducting capacity of the myocytes is slow, but certain specialized cells propagate the electrical transmissions through the heart, which leads to synchronous contraction and relaxation, as demonstrated already in 1909 (50).

Figure 1.6 shows an overview of the electrical conduction system of the heart. In the healthy heart, electrical depolarization is initiated in the *sinoatrial node* in the right atrium. The depolarization wave first expands across the atria, and subsequently reaches the *atrioventricular node* where there is a short delay in the electrical transmission, allowing the atria to fully contract. Then, the depolarization wave continues to the *Bundle of His*, which connects the atria and the septum between the left and right ventricle. The Bundle of His is divided into left and right branches, and the left branch is further split into anterior and posterior parts.

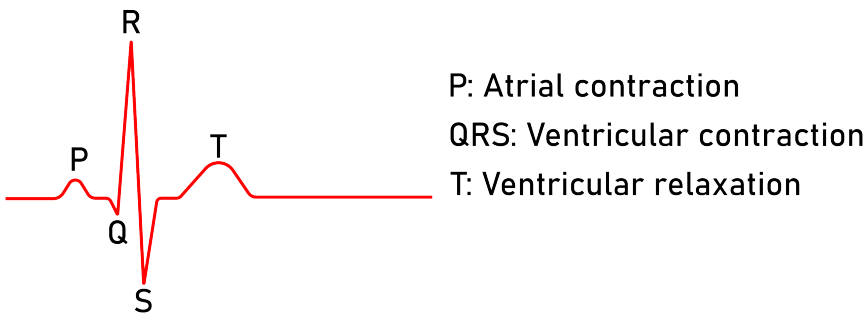

Figure 1.7: Electrocardiographic representation of atrial contraction, ventricular contraction, and ventricular relaxation.

The electrical activity of the heart can be recorded with the non-invasive examination electrocardiography (ECG). The ECG represents the sum of all the potentials of the myocytes (Figure 1.7). The resting potential is approximately -70 mV, and the maximum depolarization is determined by the equilibrium potential of sodium, which is around +55 mV. The action potential is the difference between the resting potential and the maximum depolarization potential, which is about 125 mV. The electrical activity is usually detected with the help of sticky electrodes placed on the chest, arms and legs. The voltages measured on the skin differ in magnitude across the various leads, but a normal heartbeat in a healthy heart measures approximately 0.5 mV - 4 mV on the ECG. A standard ECG consists of twelve leads, where each lead records a specific angle of the electrical activity of the heart (51). The six leads

on the chest are called precordial leads and are denoted V1-V6. The six limb leads, or extremity leads, are denoted I, II, III, aVL, aVR, and aVF.

Disturbances in the electrical conduction system can lead to dysfunctional pumping of the heart, since the muscular contraction and relaxation of the heart is dependent on efficient transmission of electrical impulses. *Left bundle branch block* is a condition where the electrical transmission through the specialized cells is slower than normal or even absent, a phenomenon which has been studied in animals and human at least since the early 1900's (52; 53; 54; 55). In left bundle branch block, the electrical impulses are instead transmitted via the non-specialized myocytes, resulting in a dyssynchronous contraction and relaxation because the electrical impulses are delayed to some parts of the heart muscle. Thus, left bundle branch block leads to a prolonged duration of systole and a relatively shorter diastolic phase of the heartbeat (56; 57). Clinical diagnosis of left bundle branch block is based on assessment with ECG (58), which shows a prolonged QRS duration of > 120 ms, broad and slurred R waves in leads I, aVL, V5 and V6, and discordant ST-T changes (Figure 1.8).

The most common underlying causes behind left bundle branch block are dilated cardiomyopathy and ischemic heart disease (59). The mechanisms behind dilated cardiomyopathy and ischemic heart disease can cause systolic and diastolic dysfunction. In addition, left bundle branch block causes dyssynchronous ventricular pumping which can impair both systolic contraction and diastolic relaxation. The combination of dyssynchronous ventricular pumping and underlying heart pathology may in time lead to reduced cardiac output and symptoms of heart failure. To assess heart function clinically, ultrasound of the heart is commonly used to measure volumes and blood flow, and evaluate the patterns of motion during ventricular contraction and relaxation.

Treatment of patients with heart failure is primarily pharmaceutical, aiming to keep the patient in the compensated stage with adequate cardiac output (2). However, some patients with heart failure and left bundle branch block may also benefit from *cardiac resynchronization therapy*, where the patient receives a special kind of pacemaker (60). The purpose of cardiac resynchronization therapy is to promote a more synchronous electrical activity, and thereby improve the pumping capacity of the heart and reduce the risk of adverse heart-failure related complications.

Despite thorough evaluation of symptoms and heart function to identify patients that are eligible for cardiac resynchronization therapy, approximately one third of patients receiving cardiac resynchronization therapy show limited or no improvement in heart function or quality of life (61; 62; 63). The purpose of Study IV was therefore to test if advanced blood-flow analysis using magnetic resonance imaging before pacemaker implantation, can improve the prediction of response to cardiac resynchronization therapy in patients that fulfill current clinical selection criteria.

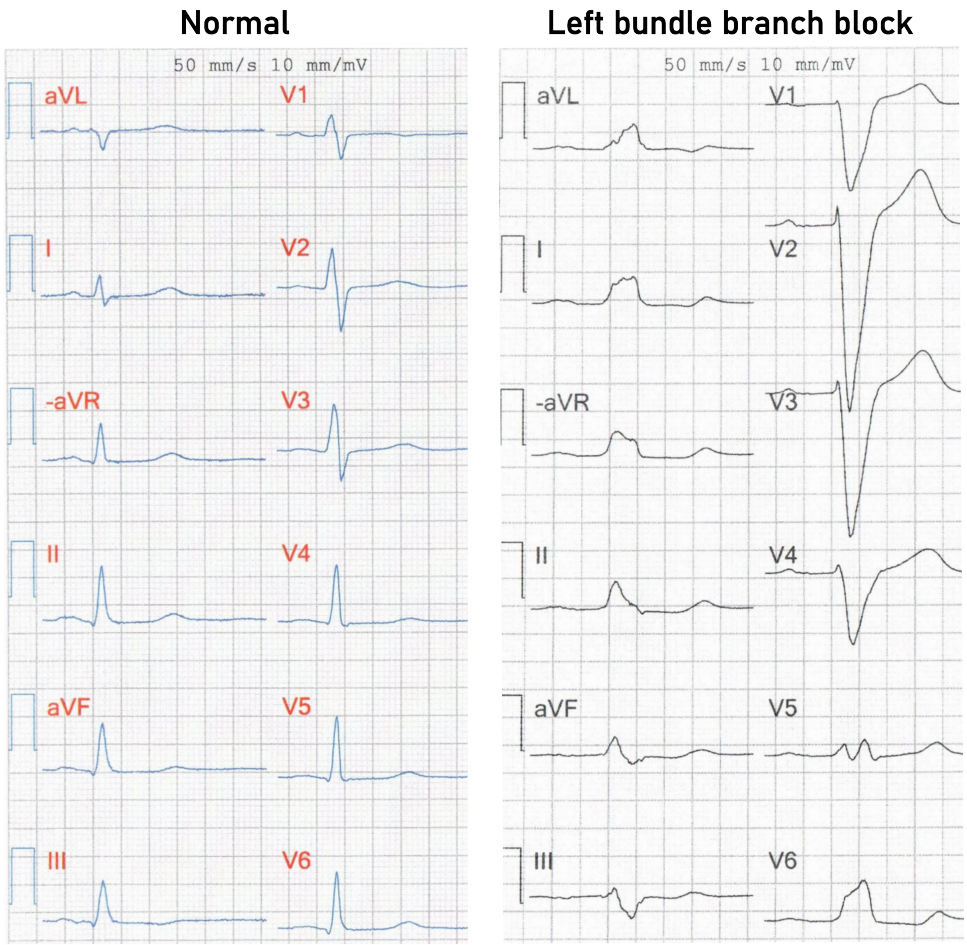

Figure 1.8: Electrocardiography in a person with a normal functioning electrical conduction system, and in a patient with left bundle branch block.

1.2 Cardiovascular magnetic resonance

Since heart failure is a condition with several possible underlying causes, thorough evaluation of heart structure and function are essential for optimal care of patients. Many people with heart conditions go undiagnosed for years, and a significant amount of previously reported cases have been shown to be misdiagnosed (64). Heart-failure phenotyping requires imaging modalities for assessing heart function in systole and diastole, at rest or at stress. However, findings are often unspecific and discovered when the heart function of the patient is already reduced. Improved understanding of the mechanics and hemodynamics in heart failure can lead to earlier and more precise detection of pathology, which may facilitate the initiation of dedicated treatment at an early stage and thereby improve the quality of life and prognosis for the individual patient.

Cardiovascular magnetic resonance imaging can provide accurate and precise evaluation of heart structures and function, including tissue characterization and assessment of blood flow in vessels and intracardiac cavities. The research projects in thesis use novel, in-house developed image-analysis methods on cardiovascular magnetic resonance imaging to evaluate cardiac mechanics and hemodynamics in patients with heart failure, specifically assessing pressure-volume relations and blood flow in the heart.

Basic physics of magnetic resonance imaging

Figure 1.9 shows a schematic illustration of the very basic principles behind magnetic resonance imaging, but the intention is by no means to provide a complete or even reality-based picture. Magnetic resonance imaging is based on the intrinsic property of some nuclei to spin, meaning rotating around their own axis. Protons spin and therefore each proton acts like a small magnet.

The behavior of protons in magnetic resonance can be explained with an analogue (65) where a group of protons act like compasses in a tumble-dryer. When a regular compass is subjected to an external magnetic field, the compass will point towards north. In magnetic resonance, a group of compasses (protons) are placed in a tumble-dryer simultaneously as they are exposed to an external magnetic field (B_0). Because of collisional energies in the tumble-dryer, all the compasses will no longer point towards north. Still, there will be a slight bias towards north, resulting in a net magnetization vector (M) aligned with the direction of B_0, commonly referred to as the z-axis.

When examining the heart with magnetic resonance imaging, the strong external magnetic field B_0 usually has a field strength of 1.5 or 3 Tesla. When B_0 is applied, the rotational axis of each spinning proton starts to perform a motion around the z-axis, also known as precessing around the direction of B_0. The precession frequency, also called the resonance frequency or the Larmor frequency, is a measure of how fast the protons rotate around the external magnetic field, and depends on the magnitude of B_0 and the gyromagnetic constant (γ) specific to each type of nucleus. The Larmor frequency is calculated using the formula:

$$Larmor\ frequency = \gamma \times B$$

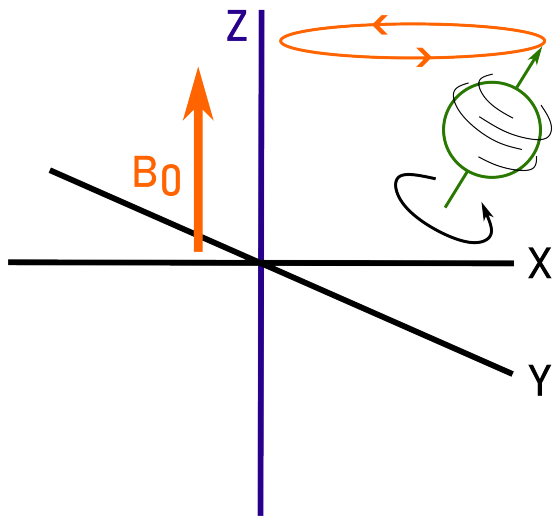

Figure 1.9: A three-dimensional coordinate system where a proton spins, meaning rotating around its own axis (green). The rotational axis of the proton precesses about a magnetic field (B_0) with a frequency called the Larmor frequency (orange).

The net magnetization vector M comprises longitudinal and transverse components. M_z represents the longitudinal component along the direction of B_0, and M_{xy} represents magnetization in the transverse plane. The magnitude of M_z depends on the field strength of B_0. In the transverse plane, the net magnetization $M_{xy} = 0$ because the spin directions of the protons are distributed evenly in the xy-plane.

To measure signals from magnetic resonance and create images, a radio-frequency pulse is introduced orthogonal to the direction of B_0. When M is aligned with B_0, the net magnetization of M cannot be measured since B_0 is significantly larger than M. The purpose of adding a radio-frequency pulse is to change the direction of the vector M, and enable measurements of the net magnetization in the xy-plane. The radio-frequency pulse is an electro-magnetic field, and the magnetic component is referred to as B_1. When the frequency of B_1 resonates with the Larmor frequency, the group of protons start to precess about B_1, resulting in an increasing net magnetization M_{xy}, and a decreasing M_z component (Figure 1.10). This process can be described as M flipping from the z-axis towards the xy-plane. The higher the field strength of B_1 and the longer the transmission time of B_1, the larger the flip angle (α) and resulting net magnetization of M_{xy}, producing a stronger detectable signal.

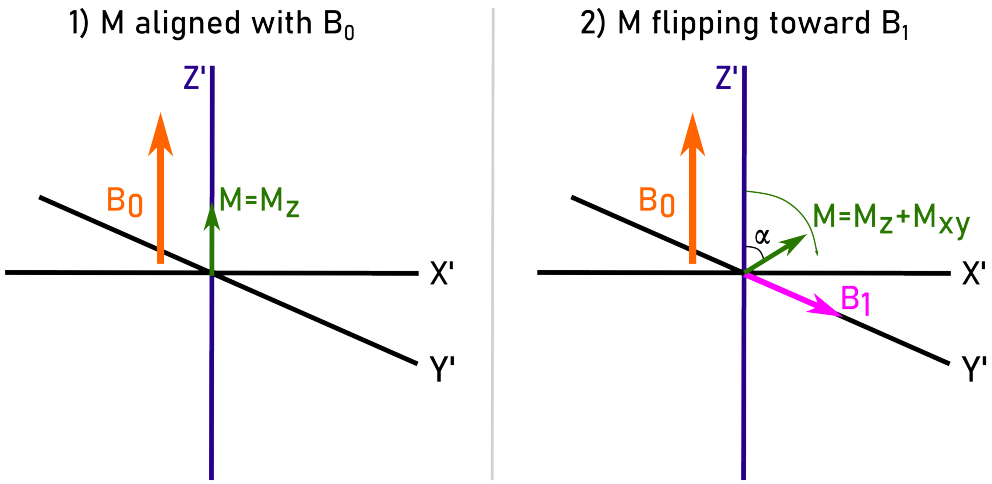

Figure 1.10: 1) When M is aligned with B_0, the net magnetization of $M=M_z$ and cannot be measured because B_0 is larger than M. 2) When a radio-frequency pulse is introduced, M starts to flip towards B_1, resulting in an increasing net magnetization in the transverse xy-plane, which can be measured. The figure shows the situations from a rotating frame of reference.

When the radio-frequency pulse ends, the vector M reverts to align with B_0 by the two independent processes *T_1 recovery* and *T_2 decay*, which happen simultaneously. T_1 recovery occurs when the group of protons no longer precess about B_1 and the spin distribution returns to the direction of B_0, resulting in an increasing longitudinal net magnetization M_z. T_2 decay is the process where the M_{xy} component decreases due to dephasing of the protons, which occurs due to interactions

between the small magnetic fields of the protons. M_{xy} also decreases due to inhomogeneities in the external magnetic field. The effective transverse decrease in net magnetization due to a combination of these processes can be measured as T_2^*. T_1, T_2 and T_2^* are influenced by the properties of the tissues, such as water content, and can be used for assessment of structural characteristics of organs. T_1 is defined as the time required for M_z to recover to 63% of its original value, and T_2 as the time required for M_{xy} to decay to 37% of its maximum value (Figure 1.11).

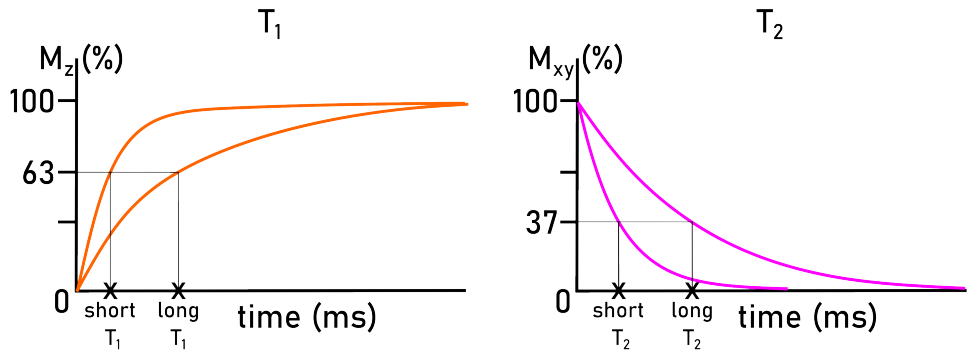

Figure 1.11: T_1 recovery is measured as the time required for M_z to return to 63% of its original value. T_2 decay is the time required for M_{xy} to decrease to 37% of its maximum value. Each graph shows examples of two tissues with different T_1 and T_2 values.

Signal localization

To create an image from magnetic resonance, the spatial positions of the protons need to be determined. Therefore, gradients are applied in three orthogonal directions, commonly referred to as x, y, and z. Note that the reference system for the spatial positions can be oriented in any direction and does not necessarily align with the three-dimensional coordinate system used to describe M_z and M_{xy}.

In the z-axis, slice selection is performed using a linear gradient. The z-gradient slightly alters the total magnetic field strength along the body, resulting in an increase in precession frequency in one end and a corresponding decrease in frequency in the other end. When radio-frequency pulses are introduced, only protons with a Larmor frequency matching the radio-frequency pulse are excited. The radio-frequency pulse has an adjustable frequency range, called bandwidth. The thickness of the slice selected is determined by the strength of the z-gradient and the bandwidth of the radio-frequency pulse.

Within the selected slice, the spatial positions of the protons need to be defined in the xy-directions. When an x-gradient is applied, the local field strength changes and thus modifies the local precession frequencies along the x-direction. The resulting signal will then consist of multiple frequencies in a complex waveform. To decode the complex waveform and extract individual components, a Fourier transform is used to compute a spectrum of frequencies from the signal. Finally, the spectrum of frequencies can be associated with the applied x-gradient to determine the spatial positions in the x-direction.

In the y-direction, the spatial positions of the protons are determined by applying a y-gradient. As variations in the magnetic field strength are introduced with the y-gradient, the protons will start to accumulate phase differences. The phase differences depend on the local field strength and the time spent in that field strength. Several experiments with y-gradients are performed serially, and the phase information is then used to determine the spatial positions of the protons in the y-direction.

ECG gating

Since the heart is a moving organ, time-resolved measurements are required for analysis of heart function. To acquire time-resolved measurements, data is commonly sampled from several heartbeats and then interpolated to represent a mean cardiac cycle. The acquired data is synchronized to the time phases of the heartbeat by gating techniques, usually based on information acquired from an ECG during the examination with magnetic resonance. Gating can be done either prospectively or retrospectively (66; 67; 68), as illustrated in Figure 1.12 and described in the following section.

In prospective gating, data acquisition starts at a trigger signal on the ECG, typically the R-wave, and continues during a fixed time period for each heartbeat (69). Prospective gating is commonly used when acquiring images for assessment of *structures*, but the motion of the heart is of less interest. Tissue characterization often include measurements of the amount of scar tissue, using the method late gadolinium enhancement, or assessment of extra-cellular volume or edema with T_1/T_2 mapping. Prospective gating can be problematic in patients with arrhythmia where the duration of the heartbeats vary a lot. In longer heartbeats, there may be a time interval in late diastole without any data acquisition. Therefore, the resulting images of a mean heartbeat may not measure late diastolic function correctly.

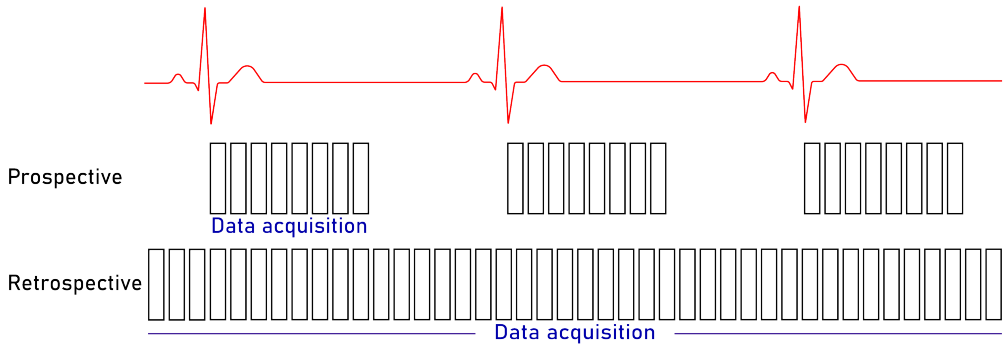

Figure 1.12: Synchronizing data to the heartbeat using ECG. In prospective gating, the data-acquisition window is pre-defined, whereas in retrospective gating, data is acquired continuously and then sorted into the time phases of the heartbeat.

In retrospective gating, data acquisition is performed continually for several heartbeats, combined with information from the ECG (70). The data is then sorted into time phases to construct time-resolved images of a mean heartbeat. Retrospective gating is commonly used when acquiring images for evaluation of the *function* of the heart, such as cine images of short- and long-axis views to assess the pumping of the heart, or images for blood-flow measurements throughout the heartbeat, described in more detail in the following sections.

Anatomical imaging

To acquire time-resolved images of the heart with a high contrast between the blood and the myocardium, a commonly used technique is balanced steady state free precession (bSSFP). The signal intensity in bSSFP is proportional to the T_2/T_1 ratio. Since blood has a higher T_2/T_1 ratio than the myocardium, the bSSFP generates images where the blood is bright and the myocardium is darker. On the one hand, the bSSFP technique offers a high signal-to-noise ratio and is thereby ideal for anatomical measurements, but on the other hand, bSSFP is sensitive to B_0 inhomogeneities and may result in image artifacts in for example patients with a pacemaker.

Flow

The most common technique for blood-flow measurements with magnetic resonance imaging is *phase-contrast sequences* (71; 72). The technique has been known since the late 1950's (73) and has been in practical use since the 1980's (74; 69; 75; 76). The idea behind phase-contrast sequences is to manipulate the precession phase of moving protons in a predictable manner, to achieve phase shifts proportional to the velocity of the protons.

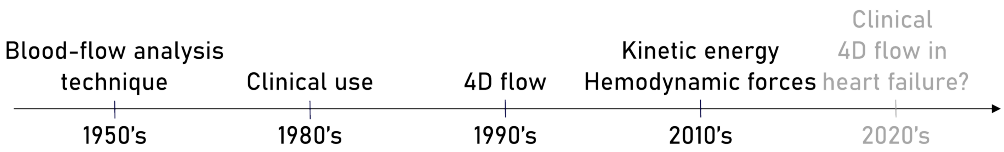

Figure 1.13: Development of blood-flow analysis with cardiovascular magnetic resonance imaging.

Figure 1.14 depicts a heavily simplified explanation of the physics behind blood-flow measurements with phase-contrast CMR. First, a gradient is applied which modifies the local magnetic field strength in a predictable manner. Thus, the protons are exposed to different field strengths depending on their spatial position. When the magnetic field strength changes, the phase of the protons will change since the phase depends on the field strength. Thereafter, the first gradient is turned off and a second gradient is applied in the opposite direction as the first one. The phase of the protons will then start to return to their original phase. The two gradients are called *bipolar gradients* since they are equal in strength but with opposite directions.

After applying a sequence of bipolar gradients, protons in stationary tissue will be in a state with unchanged phase compared to before starting the experiment. In contrast, moving protons will have accumulated phase shifts. Since the spatial positions of the moving protons will change during the experiment, a moving proton is exposed to different magnetic field strengths during the first gradient compared to during the second. The velocity of the moving protons can then be calculated from the phase shifts, also called phase contrast.

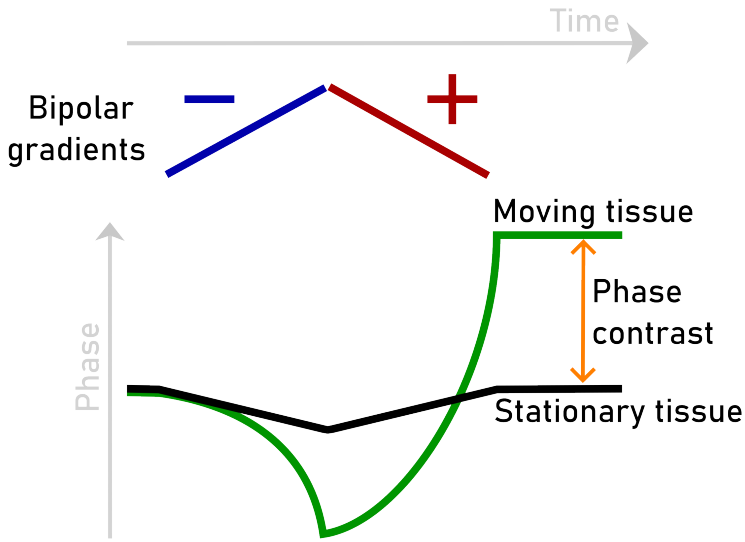

Figure 1.14: Blood-flow analysis with phase-contrast magnetic resonance imaging.

4D Flow

In clinical practice, blood-flow analysis is typically performed by applying velocity-encoding bipolar gradients in a 2D plane of interest. The position of the 2D plane is determined during data acquisition and cannot be changed retrospectively, and the resulting data depicts the blood flow orthogonal to the 2D plane. However, velocity-encoding gradients can also be applied along several spatial axes for three-dimensional, time-resolved flow measurements, called 4D flow (Figure 1.15). The techniques behind 4D flow cardiovascular magnetic resonance imaging have been developing since the 1990's (77; 78), and enable analysis of multidirectional blood flow within the cavities of the heart and adjacent large vessels (79).

When acquiring phase contrast 4D-flow data of intracardiac blood flow in adults, the spatial resolution is typically around 2.5 mm isotropic according to current recommendations (80). This spatial resolution is sufficient for blood-flow measurements, whereas images for volumetric assessment of the atria and ventricles are optimally acquired with a higher spatial resolution in images tailored for anatomical evaluation, such as bSSFP. In the analysis of 4D-flow data, the volume of interest is therefore usually defined by contouring in anatomical bSSFP images. Then, the contours are transferred to the 4D-flow data to enable blood-flow analysis of the relevant cavity, for example the left ventricle.

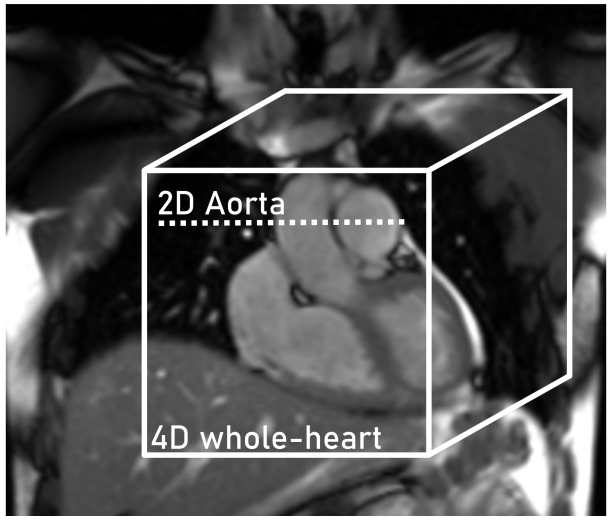

Figure 1.15: Blood flow can be analyzed from a 2D plane, here marked as a dashed line placed over the aorta, or from a 3D box covering the entire heart.

In this thesis, 4D-flow data was used to investigate novel markers for quantitative evaluation of blood flow within the heart (described in more detail in 3.4 Blood-flow analysis). The overall hypothesis behind this work was that these markers have potential to provide detailed information on the physiology and pathophysiology of the heart, and improve clinical evaluation of patients with heart failure.

Chapter 2

Aim

The overall aim of this thesis was to quantify pathological mechanisms in patients at risk for or with established heart failure, beyond the ruling paradigms of clinical heart-failure classification. The specific aims for each study were as follows:

Study I Investigate the ability of non-invasive pressure-volume loops to detect cardiac response to load alteration, by assessments at rest and during manipulation of preload and afterload in healthy hearts and in patients with hypertrophic cardiomyopathy.

Study II Investigate if 4D-flow CMR with hemodynamic-force analysis can provide new insights in right and left ventricular mechanisms in patients with precapillary pulmonary hypertension.

Study III Use 4D-flow CMR with analysis of kinetic energy and hemodynamic forces to evaluate left ventricular blood-flow patterns in patients with hypertrophic cardiomyopathy where echocardiography shows normal blood-flow measurements.

Study IV Test the performance of 4D-flow CMR with hemodynamic-force analysis for prediction of response to cardiac resynchronization therapy in patients with heart failure and left bundle branch block.

Chapter 3

Materials and methods

3.1 Study populations

This thesis is based on four studies, where Studies I and IV are post-hoc analyses of previous prospective studies, and Studies II and III are retrospective observational studies. Patients at risk for, or with established heart failure were recruited from clinical referrals. Studies I and III are collaborations with international research groups and include patients with hypertrophic cardiomyopathy evaluated at Rigshospitalet, Copenhagen (n=14, Study I), and at the University of Oxford (n=70, Study III). Studies II and IV are in-house projects and include patients with pulmonary hypertension (n=20, Study II) and patients with heart failure and left bundle branch block (n=22, Study IV) evaluated at Skåne University Hospital, Lund.

For reference values, healthy participants were recruited in Oxford (n=8 in Study I, and n=20 in Study III), Copenhagen (n=24 in Study I), and in Lund (n=12 in Study II, and n=8 in Study IV) and matched for age and sex to the patient cohorts when possible.

3.2 Study designs

Study I

This study is comprised of two sets of experiments, where alterations in preload and afterload were studied on non-invasive pressure-volume loops in groups of controls, patients with hypertrophic cardiomyopathy, and volunteers.

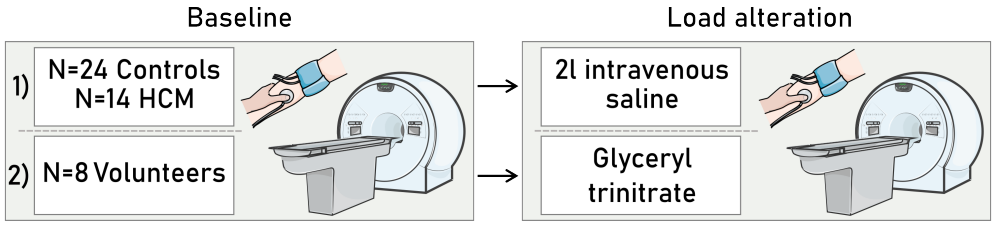

Figure 3.1: Non-invasive pressure-volume loops measured at baseline and during load alteration. 1) Controls and patients with hypertrophic cardiomyopathy were administered with intravenous saline, as previously described (81; 82). 2) Healthy volunteers was administered with continuous infusion of glyceryl trinitrate (83).

First, controls (n=24) and patients with hypertrophic cardiomyopathy (n=14) were examined at baseline with cardiovascular magnetic resonance imaging and non-invasive brachial blood-pressure measurements. The two groups then exited the scanner and received intravenous administration of isotonic saline (0.9%), with a median volume of 1.5 L during approximately half an hour. Then, participants were re-examined during load alteration, while receiving an additional 0.5 L of saline.

Secondly, healthy volunteers (n=8) were examined with cardiovascular magnetic resonance imaging and brachial blood-pressure measurements at baseline and during load alteration with glyceryl trinitrate in one imaging session. Glyceryl trinitrate was administered at 1 mg/ml at a rate of 3 ml/h, and titrated to a target mean arterial pressure reduction of 15 mmHg.

Study II

This study investigated new markers of right and left ventricular patophysiology in patients with pulmonary arterial hypertension and in patients with chronic thromboembolic pulmonary hypertension, together grouped as *precapillary pulmonary hypertension* (PH_{precap}).

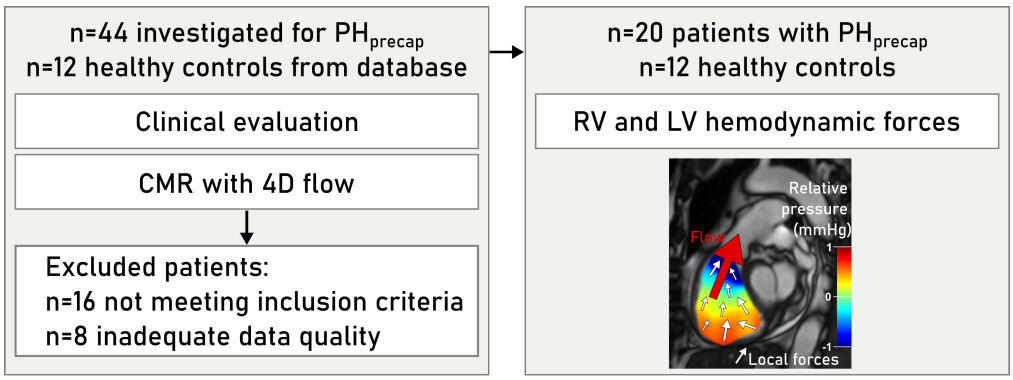

Figure 3.2: Patients with suspected precapillary pulmonary hypertension (PH_{precap}) underwent clinical evaluation and cardiovascular magnetic resonance (CMR) imaging with 4D flow. The final analysis of n=20 patients and n=12 controls included right (RV) and left (LV) ventricular hemodynamic forces, volumes, mass, atrioventricular plane displacement, and strain.

Patients underwent clinical evaluation, including invasive measurements of pressure and resistance with right-heart catheterization, as well as cardiovascular magnetic resonance imaging with 4D flow. From the 4D-flow data, right and left ventricular relative pressure gradients were computed for analysis of hemodynamic forces. For comparison, twelve healthy controls were included, matched for age and sex to the patient cohort.

Study III

In this study, patients with hypertrophic cardiomyopathy (HCM) and normal flow measurements on echocardiography were evaluated with cardiovascular magnetic resonance with 4D flow, to search for potential novel markers of heart dysfunction in this patient cohort.

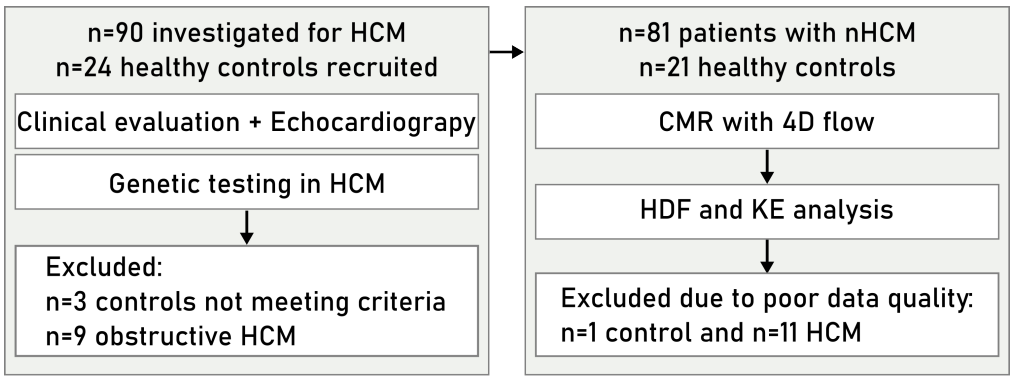

Figure 3.3: Patients investigated for hypertrophic cardiomyopathy (HCM) underwent clinical evaluation, echocardiography and genetic testing. Based on the measurements from echocardiography, non-obstructive patients (nHCM) were selected and examined with cardiovascular magnetic resonance (CMR) with 4D flow. From the 4D-flow data, left ventricular hemodynamic forces and kinetic energy were computed. Furthermore, CMR image analysis also included left ventricular volumes, mass, wall thickness, stroke work from non-invasive pressure-volume loops, and fibrosis assessment from late gadolinium enhancement.

Patients investigated for HCM underwent clinical evaluation including mapping of any family history of HCM. Echocardiography was performed to measure left-ventricular outflow-tract pressure gradients and select patients with a non-obstructive profile. Genetic testing was completed according to clinical routines for examination of genotype status. From cardiovascular magnetic resonance imaging, left ventricular hemodynamic forces and kinetic energy were computed. For comparison, n=20 healthy controls were included.

Study IV

This study investigated if patients with heart failure and left bundle branch block can profit from examination with cardiovascular magnetic resonance imaging with 4D flow for prediction of response to *cardiac resynchronization therapy* (CRT).

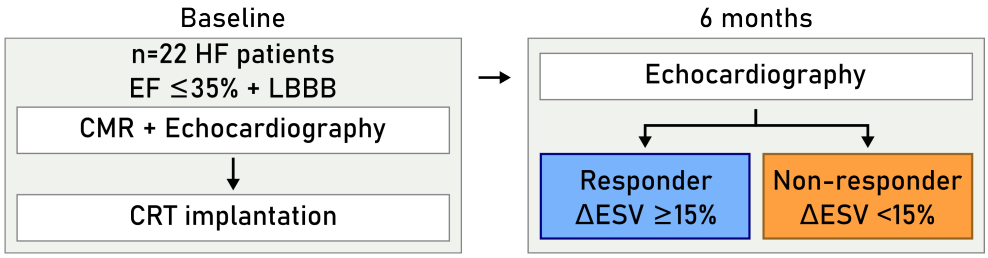

Figure 3.4: Patients with heart failure (HF), ejection fraction $\leq$ 35% and left bundle branch block (LBBB) were examined with cardiovascular magnetic resonance imaging (CMR) and echocardiography before implantation of a biventricular pacemaker for *cardiac resynchronization therapy* (CRT). At six-months follow-up after pacemaker implantation, patients were examined again with echocardiography and categorized as responders if they had an end-systolic volume (ESV) reduction of 15% or more, or non-responders if less than 15% ESV reduction. To test the predictive value of CMR with 4D flow for CRT response, left ventricular hemodynamic forces were computed from the baseline examinations, and analyzed in relation to outcome data.

The study included patients with heart failure and left bundle branch block eligible for CRT, based on standard clinical evaluation. All patients had previously been included as a part of the study cohort in a prospective study evaluating CRT outcome (84). At baseline, patients underwent echocardiography as well as cardiovascular magnetic resonance with 4D flow, before pacemaker implantation. At six-months follow up after pacemaker implantation, patients were again examined with echocardiography to evaluate response to CRT. Then, data analysis was performed to investigate the value of left ventricular hemodynamic forces computed from 4D flow data at baseline, for prediction of CRT response at six-months follow-up.

3.3 Pressure-volume analysis

Non-invasive left ventricular pressure-volume loops were calculated from volumetric data measured on standard CMR images, combined with non-invasive brachial blood-pressure measurements, using the software Segment (85; 86). This non-invasive method is developed in our research group and has been tested against invasive measurements in experimental models (14; 15) and in human (16).

Left ventricular volumes and mass were measured in end-diastole and end-systole by manual contouring of endocardial and epicardial borders in cine short-axis bSSFP images. Then, automatic interpolation of left ventricular volumes were performed throughout the entire cardiac cycle, with manual adjustments where needed. Peak systolic pressures were calculated based on systolic (SBP) and diastolic (DBP) brachial blood-pressure measurements, using the following formula (87):

$$Peak\ systolic\ pressure \approx 0.83 \times SBP + 0.15 \times DBP$$

End-diastolic pressures were estimated to 7.5 mmHg in all studies, based on previous work assessing end-diastolic pressures assumptions between 0-15 mmHg, showing a negligible impact on the resulting pressure-volume loop parameters (14). Left ventricular pressures were estimated from a time-varying elastance model, scaled in amplitude based on the non-invasive brachial blood-pressure measurements, and in time relating to the smallest and largest ventricular volumes, as previously described in detail (14). From the resulting pressure-volume loops, as visualized in Figure 3.5, parameters on cardiac mechanics and hemodynamics were calculated for Studies I and III.

Pressure-volume loop parameters related to end-systolic pressure-volume relationship included left ventricular contractility, arterial elastance and ventricular-arterial coupling. Contractility was calculated in mmHg/ml as the slope of the line defined from the two points E_{max} and V_0, where E_{max} is the point of maximum elastance, and V_0 is the theoretical volume when the intraventricular pressure is zero, here assumed $V_0 = 0$. Arterial elastance was calculated in mmHg/ml as the slope of the line defined from the two points E_{max} and the end-diastolic volume intercept on the x-axis. Ventricular-arterial coupling was calculated as the ratio between arterial elastance and contractility.

Parameters related to ventricular work included stroke work, potential energy and ventricular efficiency. Stroke work was measured in Joule as the area of the loop,

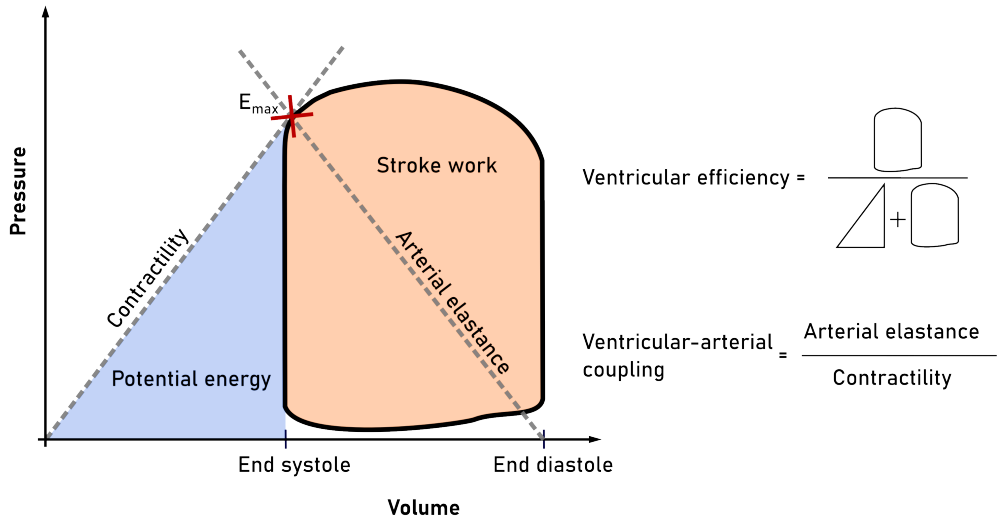

Figure 3.5: Parameters on cardiac mechanics and hemodynamics calculated from non-invasive pressure-volume loops.

and potential energy in Joule as the area of the triangle encompassed by the x-axis, the contractility slope, and the left side of the pressure-volume loop. Ventricular efficiency was defined in % as the ratio between stroke work and the sum of potential energy and stroke work.

3.4 Blood-flow analysis

Blood-flow analysis from 4D-flow cardiovascular magnetic resonance imaging was the primary research method used in Studies II, III and IV. All image analysis was performed using the software Segment (85; 86). Prior to all 4D-flow analysis, data was reviewed and processed to ensure adequate image quality. Each 4D-flow data set was assessed visually in all three phase-encoding directions, to inspect the data regarding noise and artifacts. Residual phase offsets were adjusted for using background correction fitting to stationary tissue (88; 89). Aliasing was corrected for using automatic unwrapping (90; 91). The spatial position of the 4D flow data was manually adjusted to align with the bSSFP cine short-axis images if needed. After contouring the left and right ventricular cavities over the cardiac cycle, as described in Chapter 3.3, the contours were extrapolated to the 4D-flow data, and hemodynamic forces and kinetic energy were computed.

Hemodynamic forces

Hemodynamic forces reflect the forces between the blood pool in the heart and the surrounding myocardium. In several conditions of heart failure, hemodynamic forces have been shown to differ compared to healthy controls, but the clinical value has been debated (92; 93; 94; 95; 96). As of today, hemodynamic-force analysis is predominately used for research purposes and can be measured using various modalities, including echocardiography (97) and magnetic resonance imaging (98; 99; 94; 100). In the research projects in this thesis, hemodynamic forces were quantified from 4D-flow magnetic resonance imaging in Studies II, III and IV, in the left and right ventricles in patients with various phenotypes of heart failure.

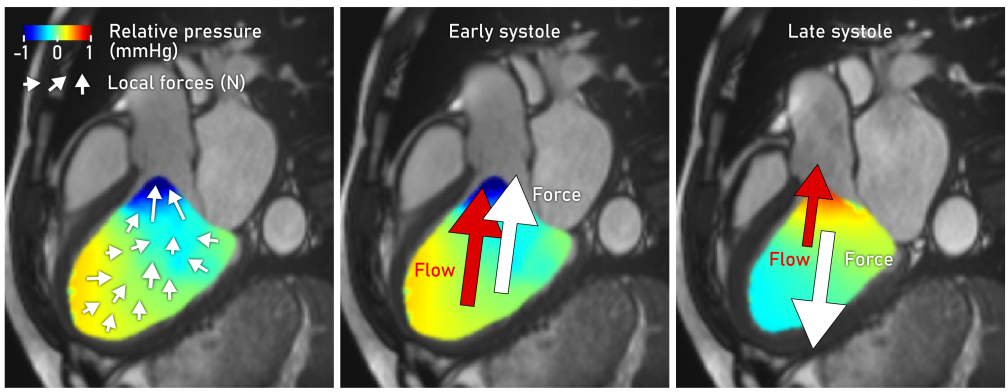

Figure 3.6: Visualization of hemodynamic forces in the left ventricle in early and late systole. Relative pressure gradients within the ventricle were computed from 4D-flow cardiovascular magnetic resonance, shown here as a colored field. The small white arrows illustrate the local hemodynamic forces, which are computed from the field of pressure gradients. The large white arrow is the global hemodynamic force, which is a sum of all the smaller local forces. The red arrow shows the blood flow, which in early systole accelerates towards the aorta, in concordance with the direction of the global force. In late systole, the direction of the global force is opposite to the direction of the blood flow, meaning that the blood is still flowing towards the aorta but decelerating.

When the ventricle contracts and relaxes, pressure gradients are created and the blood accelerates according to Newton's second law of motion (Force = mass x acceleration). Simultaneously, the blood exerts counter-forces upon the surrounding myocardium, according to Newton's third law of motion (stating that for every action, there is an equal and opposite reaction). These forces can be measured as hemodynamic forces, and are determined by the moving walls of the ventricle and the valves, as well as the more external pressures in the large vessels and the atrium. To analyze the hemodynamic forces quantitatively, pressure gradients within the left and right ventricles of the heart were computed from the 4D-flow data using the

Navier-Stokes equations. Local forces were computed for each three-dimensional voxel, and the global hemodynamic force was calculated as a sum of all the small local forces.

To evaluate three-dimensional hemodynamic-force patterns, a spatial reference system was used, as visualized in Figure 3.7. First, the atrio-ventricular plane was defined by manually placing eight points in the three long-axis cine images in the end-diastolic time-phase. For the left ventricle, the longitudinal direction (apex-base) was then set perpendicular to the atrio-ventricular plane. Two transverse directions were set parallel to the atrio-ventricular plane, where one direction (lateral wall-septum) was aligned with the left-ventricular outflow tract, and the other transverse direction (inferior-anterior) was set perpendicular to the first. The right-ventricular reference system was identical to the one in the left ventricle, but renamed to depict the anatomical landmarks on the right side of the heart.

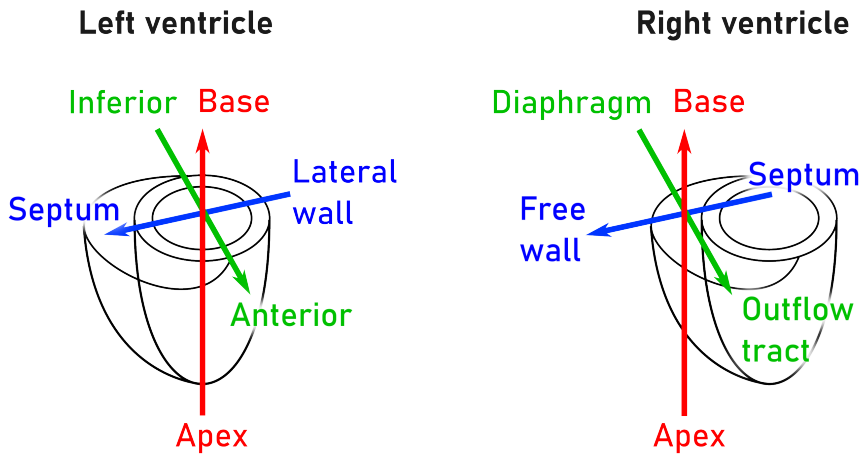

Figure 3.7: A three-dimensional spatial reference system for analysis of hemodynamic forces in the left and right ventricle.

To compare hemodynamic forces between patients with different heart rates and thus different lengths of one heartbeat, a common time axis was created with time measured in % of the total heartbeat. Furthermore, linear resampling was performed to maintain the proportion of systole and diastole in relation to the duration of the heartbeat, using end diastole and end systole as temporal landmarks.

Assessment of hemodynamic forces was performed by calculation of mean and peak values in systole and diastole, combined with visual interpretation of the time-resolved force patterns covering the entire heartbeat. To facilitate comparison of force magnitudes regardless of vector polarity, root-mean-square values were calculated. The proportion between longitudinal and transverse forces was analyzed, where the healthy heart typically exhibits predominant longitudinal forces, using a fore-ratio calculation as follows:

$$Force\ ratio = \frac{\sqrt{(lateralwall - septum)^2 + (inferior - anterior)^2}}{apex - base}$$

Kinetic energy

The energy of the blood due to motion can be quantified as kinetic energy, and measured using 4D-flow cardiovascular magnetic resonance imaging. Kinetic energy has previously been measured in the healthy heart and in patients with different phenotypes of heart failure, both as a sum of the total kinetic energy within a heart chamber of interest (101; 102; 103; 104; 105; 106; 96), and as functional components for assessment of the determinations of blood-flow patterns (107; 108; 109; 110; 111). In this thesis, left ventricular kinetic energy was evaluated in patients with hypertrophic cardiomyopathy in Study III, by computing mean and peak values for systole, early diastole and late diastole. Kinetic energy was measured in every voxel of the left ventricle using the following formula:

$$Kinetic\ energy = \frac{mass \times velocity^2}{2}$$

The mass of the blood pool was defined by multiplying the volume, measured from endocardial short-axis contours as described in Chapter 3.3, with an assumed blood density of 1.05 g/cm³ (112). The global ventricular kinetic energy of the blood in each time phase was calculated as a sum of the kinetic energy in all voxels.

3.5 Echocardiography

Echocardiography was performed as a part of the routine clinical examination of all patients in studies I-IV. Study-specific echocardiography was perdormed in Study III in patients with suspected hypertrophic cardiomyopathy, and in Study IV in patients with heart failure and left bundle branch block. To visualize the inner organs of the body, echocardiography uses ultrasound waves that can penetrate many structures in the body. The penetration capacity and image quality depends on the frequency of the ultrasound waves, where lower frequencies can reach deeper into the body, but higher frequencies result in images with higher resolution. For standard adult heat imaging, transthoracic echocardiography typically uses frequencies of 2-5 MHz (113). In clinical practice, echocardiography with two-dimensional imaging and Doppler are the most commonly used methods to assess the function, volumes and blood flow of the heart (113).

In the research projects in this thesis, transthoracic echocardiography was used to assess pressure gradients in the left ventricular outflow tract, and to measure parameters used for evaluation of left ventricular systolic and diastolic function. In Study III, pressure gradients were measured at rest and after Valsalva maneuver, and were used to evaluate if the patient has an obstructive left ventricular outflow tract, defined as a pressure-gradient > 30 mmHg. Only patients *without* left ventricular outflow tract obstruction were included in Study III. Pressure-gradients were calculated using the following formula:

$$\Delta\ Pressure = 4 \times velocity^2$$

To evaluate diastolic function in Study III, pulsed-wave Doppler was used to measure blood flow, and tissue Doppler was used to measure the movement of the atrio-ventricular plane during filling of the left ventricle. Specifically, pulsed-wave Doppler was used for trans-mitral measurements of early and late diastolic filling velocities, and tissue Doppler was used for measurements of early diastolic lateral and septal mitral annular velocities. In Study IV, systolic function was assessed by standard echocardiographic measures of left ventricular volumes using the Simpson's biplane method, to identify patients who met the inclusion criterion of an ejection fraction $\leq 35\%$.

3.6 Cardiac resynchronization therapy

Study IV included patients with heart failure and left bundle branch block who received *cardiac resynchronization therapy* with a biventricular pacemaker on clinical indications. The idea behind cardiac resynchronization therapy is to improve heart function by synchronizing ventricular contraction and relaxation. In patients with left bundle branch block, the depolarization of the left ventricular lateral wall is delayed due to a blockage in the electrical transmission pathway. Consequently, the lateral wall contracts after the septum, and thereby also relaxes after the septum. The disturbed electrical conduction system thus leads to inefficient pumping. To facilitate synchronous contraction of the ventricles, the biventricular pacemaker uses three leads; one in the right atrium, one in the apex, and one lead in the coronary venous system close to the left ventricular lateral wall.

Cardiac resynchronization therapy has been shown to improve heart function and reduce the symptoms of heart failure and the occurrence of hospitalization and death (114; 115). However, approximately one-third of patients show limited improvements six months after receiving cardiac resynchronization therapy, despite meeting current selection criteria on ECG and echocardiography, also including receiving optimal medical treatment (62). Therefore, new diagnostic markers are needed for improved prediction of response to cardiac resynchronization therapy. Previous studies have identified wider QRS-duration, sinus rhythm, non-ischemic cardiomyopathy, and female sex as predictors associated with positive outcome. In this thesis, Study IV investigated the potential of cardiovascular magnetic resonance with 4D-flow analysis as a complementary diagnostic instrument to current clinical selection criteria for better prediction of response to cardiac resynchronization therapy.

3.7 Statistics and figures

Statistical analyses were performed using GraphPad Prism (GraphPad Software, Boston, Massachusetts, USA), R (Integrated Development for R. RStudio, PBC, Boston, Massachusetts, USA), and SPSS (Armonk, NY: IBM Corp). Continuous data is presented as median and inter-quartile range [IQR], or mean and standard deviation (SD), and categorical data as absolute numbers and proportion (%). The Student's t-test or the Mann-Whitney U test were used to compare unpaired continuous data between groups, and the Wilcoxon test was used for paired comparisons. Fisher's exact test was used to compare binary categorical data.

Correlations were assessed using the Pearson or Spearman correlation test to calculate a correlation coefficient (r), and associations were analyzed from simple and multiple linear regressions with computation of a coefficient of determination (R^2). A multivariate logistic regression was performed to analyze the relationship between independent and dependent variables. The Bland-Altman analysis was used for evaluation of method agreement (116; 117). A receiver operating characteristic (ROC) analysis was used to evaluate the predictive performance of hemodynamic-force analysis for response to cardiac resynchronization therapy response (Study IV). In all studies, a two-tailed p-value < 0.05 was considered significant. When multiple statistical tests were performed, the cut-off p-value for statistical significance was adjusted by dividing the p-value 0.05 by the number of tests.

4D-flow data was visualized as intraventricular fields of kinetic energy and pressure-gradients, using plug-ins in the software Segment (Medviso, Lund, Sweden) (85). Graphs presenting the results were generated using GraphPad Prism (GraphPad Software, Boston, Massachusetts, USA). Figures were prepared using Inkscape (The Inkscape Project, https://inkscape.org/).

Chapter 4

Results and comments

4.1 Study I

The data in Study I demonstrate alterations in preload and afterload evaluated on non-invasive pressure-volume loops in healthy participants and in patients with hypertrophic cardiomyopathy (HCM).

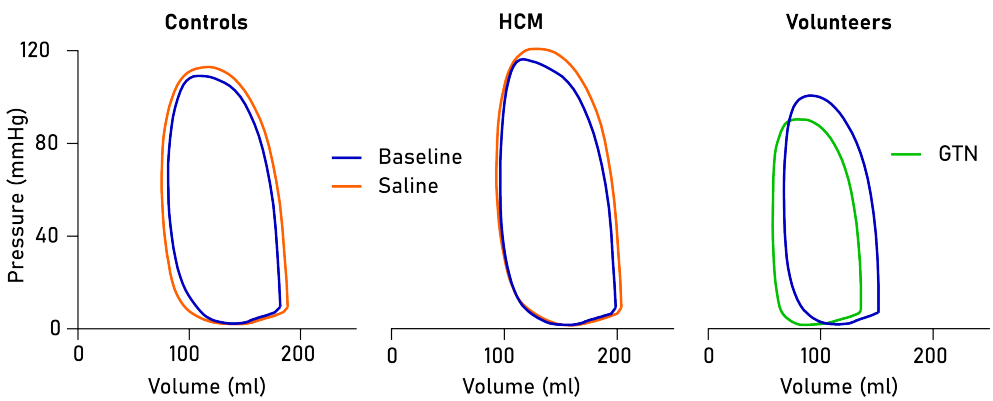

Figure 4.1: Average pressure-volume loops before and during load alteration with saline in controls and in patients with hypertrophic cardiomyopathy (HCM), and with glyceryl trinitrate (GTN) in volunteers.

Saline infusion

Controls and patients with HCM responded differently to saline infusion, as shown on parameters calculated from non-invasive pressure-volume loops (Figure 4.2). During load manipulation with saline, arterial elastance and potential energy decreased in controls but not in HCM. In both groups, ventricular-arterial coupling decreased, and stroke work and ventricular efficiency increased, while contractility remained unchanged. Visual assessment of the average pressure-volume loops showed an increased area of the loops in both groups during load alteration (Figure 4.1). In controls, the area increased mainly due to volumetric changes, with an increased end-diastolic volume and a decreased end-systolic volume, whereas in patients with HCM the increased area was primarily due to increased pressures and end-diastolic volume.

Glyceryl trinitrate infusion

Figure 4.3 shows decreased stroke work and potential energy in volunteers during infusion with glyceryl trinitrate, suggesting unloading of the ventricle. Congruently, visual assessment of the average pressure-volume loops shows a left-ward shift of the loops during load alteration, in combination with a decreased hight of the loop due to lower pressures (Figure 4.1). Glyceryl trinitrate infusion did not lead to statistically significant changes in contractility, arterial elastance, ventricular-arterial coupling, or ventricular efficiency.

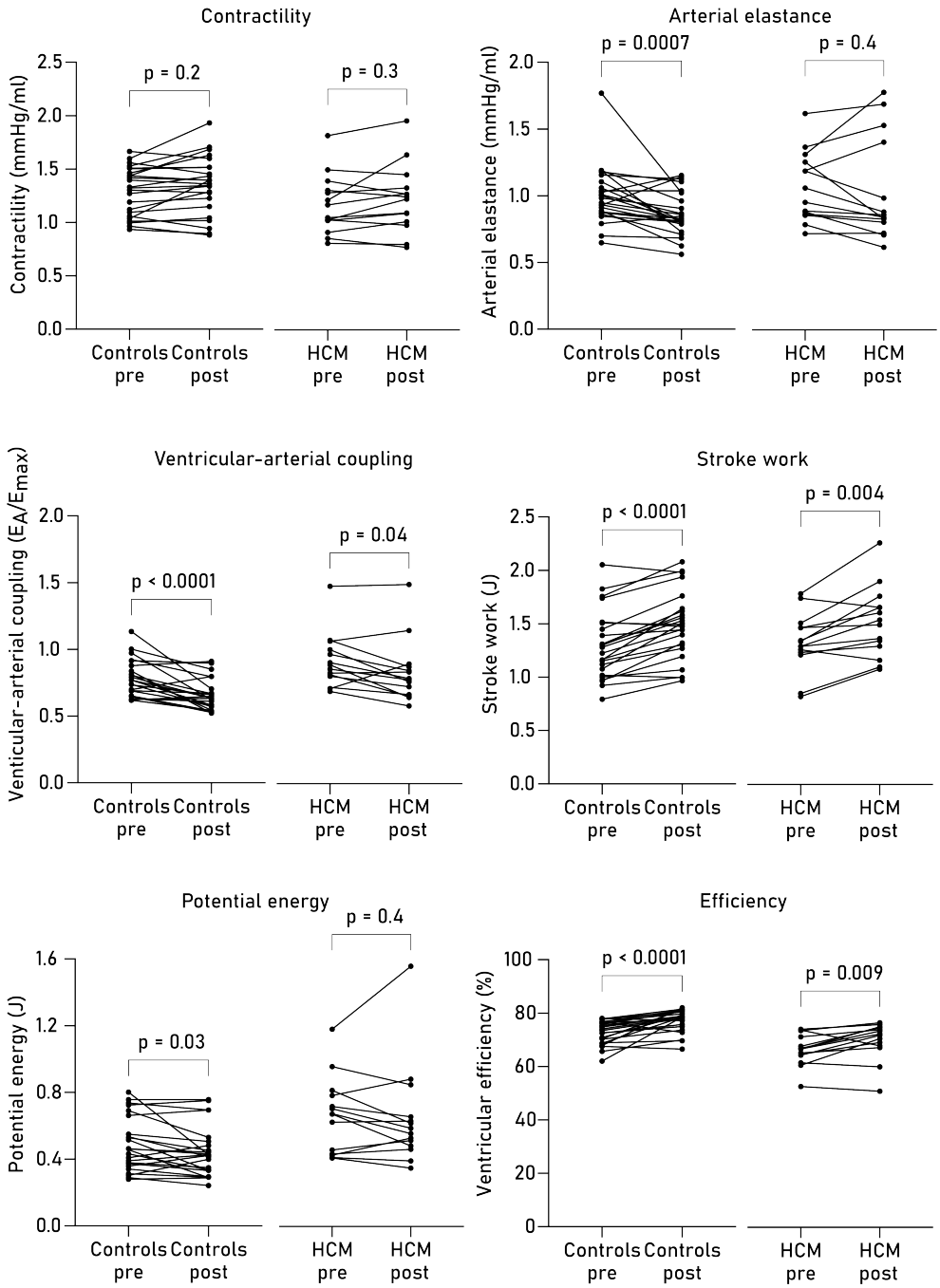

Figure 4.2: Pressure-volume loop parameters in controls and in patients with hypertrophic cardiomyopathy (HCM) at baseline (pre) and during infusion of isotonic saline (post).

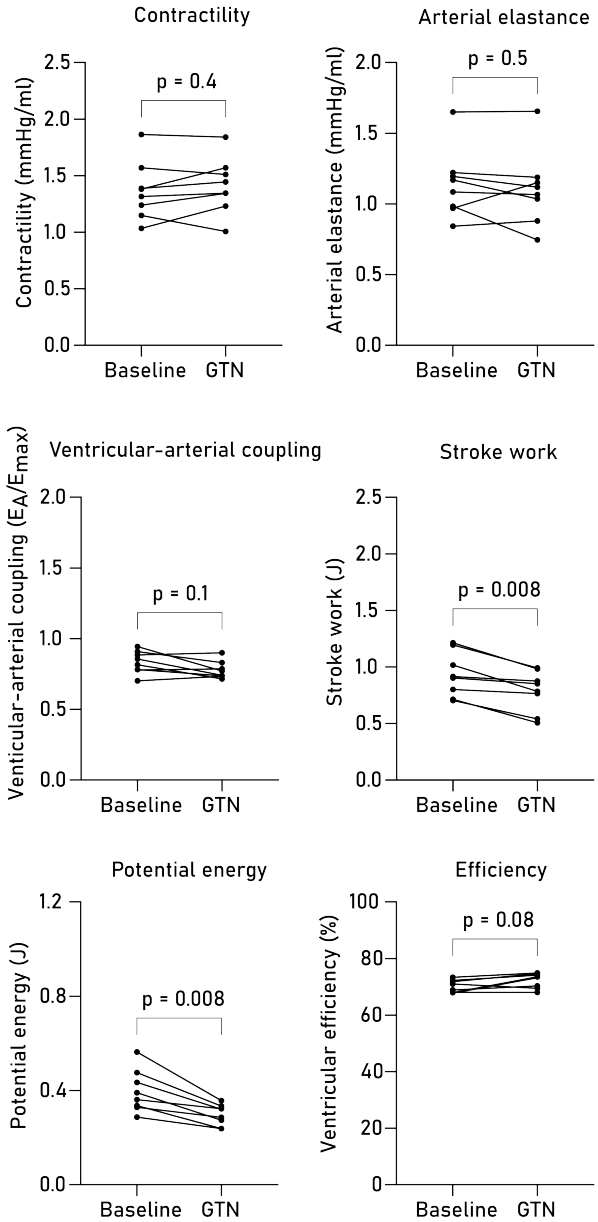

Figure 4.3: Pressure-volume loop parameters in volunteers at baseline and during infusion of glyceryl trinitrate (GTN).

4.2 Study II

The results in Study II show that in patients with precapillary pulmonary hypertension (PH_{precap}), the right ventricle acts more like a pressure pump than a volume pump, as opposed to healthy controls. In patients with PH_{precap}, hemodynamic forces measured from 4D flow cardiovascular magnetic resonance imaging were higher in both the right and left ventricle, compared to controls matched for age and sex.

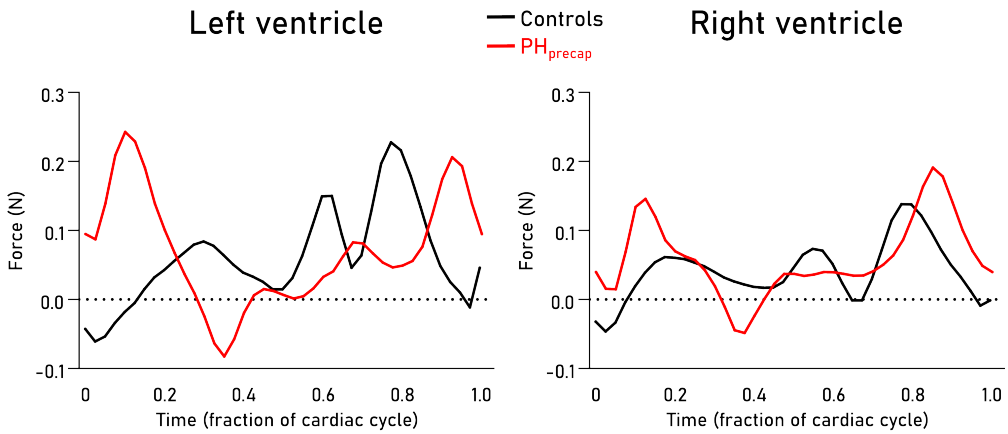

Figure 4.4: Longitudinal hemodynamic forces (apex-base direction) in the left and right ventricle in controls and in patients with precapillary pulmonary hypertension (PH_{precap}). The force data is presented as the mean value for controls and patients respectively in each time point.

Right ventricle

Systolic right ventricular hemodynamic forces indexed to stroke volume were higher in the transverse directions in patients with PH_{precap} compared to controls (Figure 4.5). Moreover, patients with PH_{precap} had lower atrioventricular plane displacement compared to controls, meaning a shorter longitudinal movement of the ventricle during contraction and relaxation, which is in keeping with previous studies (118; 119). Still, stroke volumes were similar in the right ventricle when comparing patients and controls. These results indicate that in patients with PH_{precap}, the right ventricle pumps with more transverse ventricular motion to overcome the increased right ventricular afterload and maintain stroke volume, as opposed to the predominant longitudinal ventricular motion seen in healthy hearts (120; 121).

Diastolic right ventricular hemodynamic forces were higher in patients with PH_{precap} compared to controls in both the longitudinal and transverse directions (Figure 4.6). Visual interpretation of the time-resolved hemodynamic-force data show that on the group level, controls exhibit two peaks in diastole corresponding to early filling and atrial contraction (Figure 4.4), in keeping with previous studies (122; 93). On the contrary, patients with PH_{precap} present with *one* main force peak, occurring in the late diastolic phase corresponding to atrial contraction. Indeed, previous studies have shown that patients with pulmonary hypertension exhibit a larger contribution of atrial contraction to right ventricular filling, compared to controls (123).

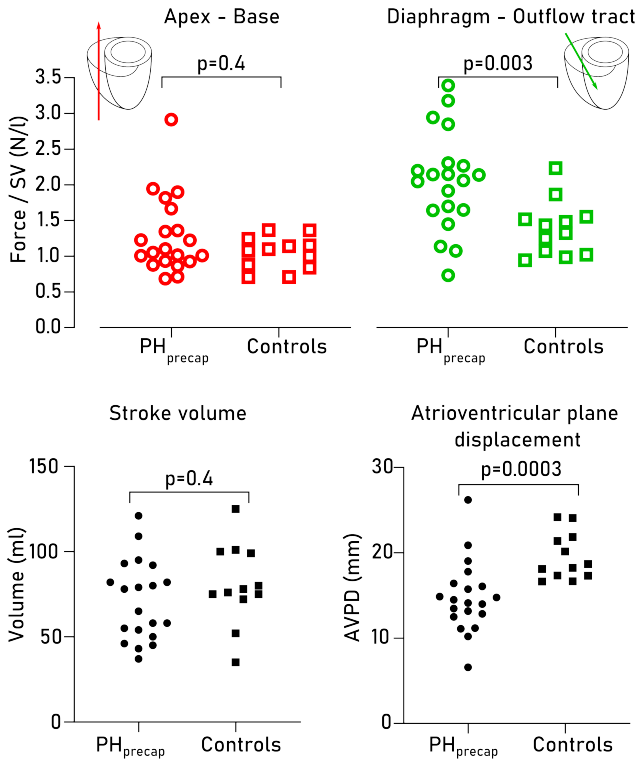

Figure 4.5: Right ventricular systolic hemodynamic forces, stroke volume (SV), and atrioventricular plane displacement (AVPD) in patients with precapillary pulmonary hypertension (PH_{precap}) and in healthy controls.

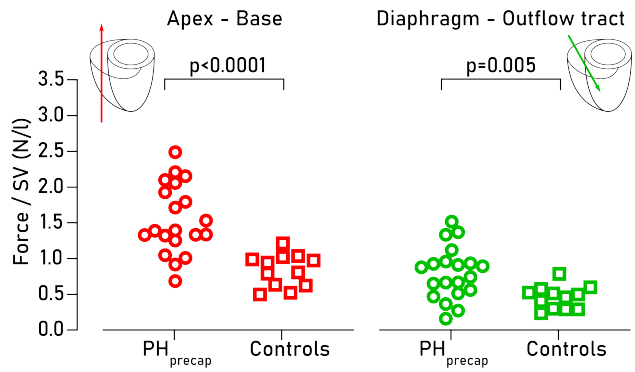

Figure 4.6: Right ventricular diastolic hemodynamic forces in patients with precapillary pulmonary hypertension (PH_{precap}) and in healthy controls.

Left ventricle

Systolic left ventricular hemodynamic forces indexed to stroke volume were higher in patients with PH_{precap} compared to controls in the longitudinal (apex-base) and the outflow (lateral wall-septum) directions (Figure 4.7). On the group level, patients had smaller stroke volumes and end-diastolic volumes compared to controls, despite similar body sizes. Aberrant hemodynamic forces and smaller left ventricular volumes could be linked to anatomical deformation of the left ventricle, where high right ventricular pressures and volumes lead to the septum bulging into the left ventricle, resulting in the left ventricle shaped like a "D". A D-shaped left ventricle in systole is primarily associated with right ventricular *pressure* overload, whereas a diastolic D-shape suggests right ventricular *volume* overload (124). Septal flattening was seen in systole in about 1/3 of patients, and in diastole in all patients but to different extents. Moreover, the hearts of patients may be driven by a higher sympathetic stimulation, as suggested from higher heart rates, with increased left ventricular contractility that could contribute to increased hemodynamic forces.

Diastolic left ventricular hemodynamic forces indexed to stroke volume were higher in patients with PH_{precap} compared to controls in the longitudinal direction (Figure 4.8). Visual interpretation of the time-resolved hemodynamic-force data show that on the group level, both patients and controls exhibit two peaks in diastole, but patients show a larger difference in the peak amplitudes, with a relatively smaller peak in early than in late diastole, compared to controls (Figure 4.4). Previous studies on left ventricular function in pulmonary hypertension have suggested both intrinsic left ventricular dysfunction with reduced diastolic suction (125), and left ventricular underfilling (126). In Study II, the combination of higher forces indexed to stroke volume and smaller left ventricular volumes, is likely best explained by underfilling of the left ventricle.

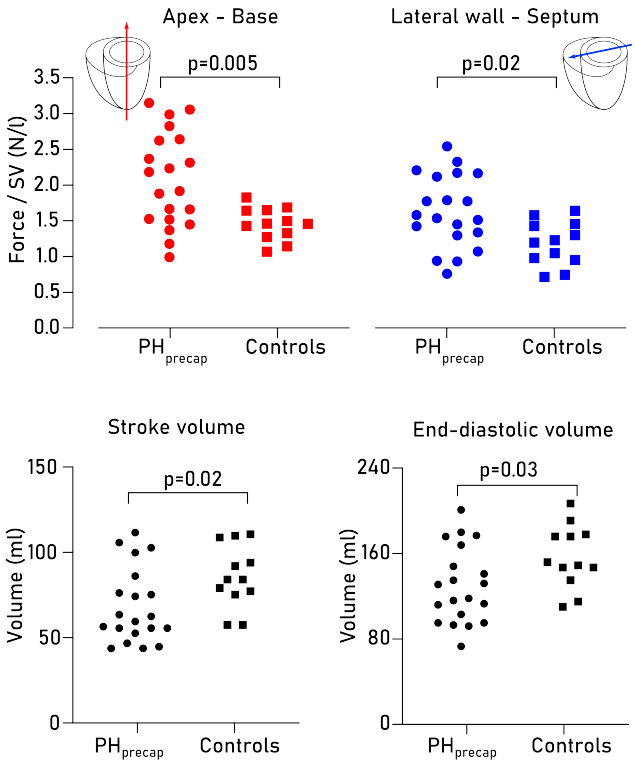

Figure 4.7: Left ventricular systolic hemodynamic forces, stroke volume (SV), and end-diastolic volume in patients with precapillary pulmonary hypertension (PH_{precap}) and in healthy controls.

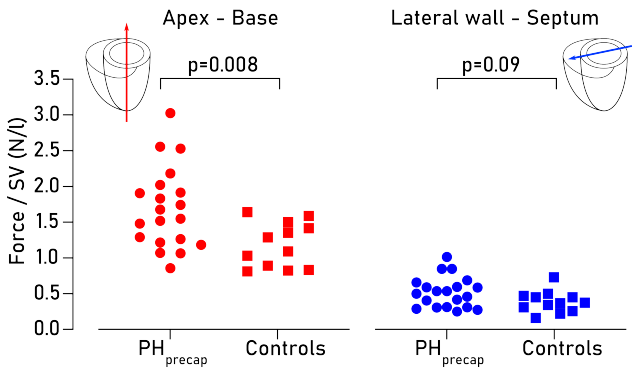

Figure 4.8: Left ventricular diastolic hemodynamic forces in patients with precapillary pulmonary hypertension (PH_{precap}) and in healthy controls.

4.3 Study III

The data in Study III demonstrate that in patients with non-obstructive hypertrophic cardiomyopathy, cardiovascular magnetic resonance with 4D flow imaging may detect hemodynamic abnormalities even when echocardiographic flow measurements are normal. The patients included in this study were in NYHA class I or II, meaning they had no or only minor symptoms of heart failure. Still, left ventricular blood flow was different in this patient cohort compared to controls matched for age and sex. Specifically, patients exhibited higher hemodynamic forces and kinetic energy in both systole and diastole.

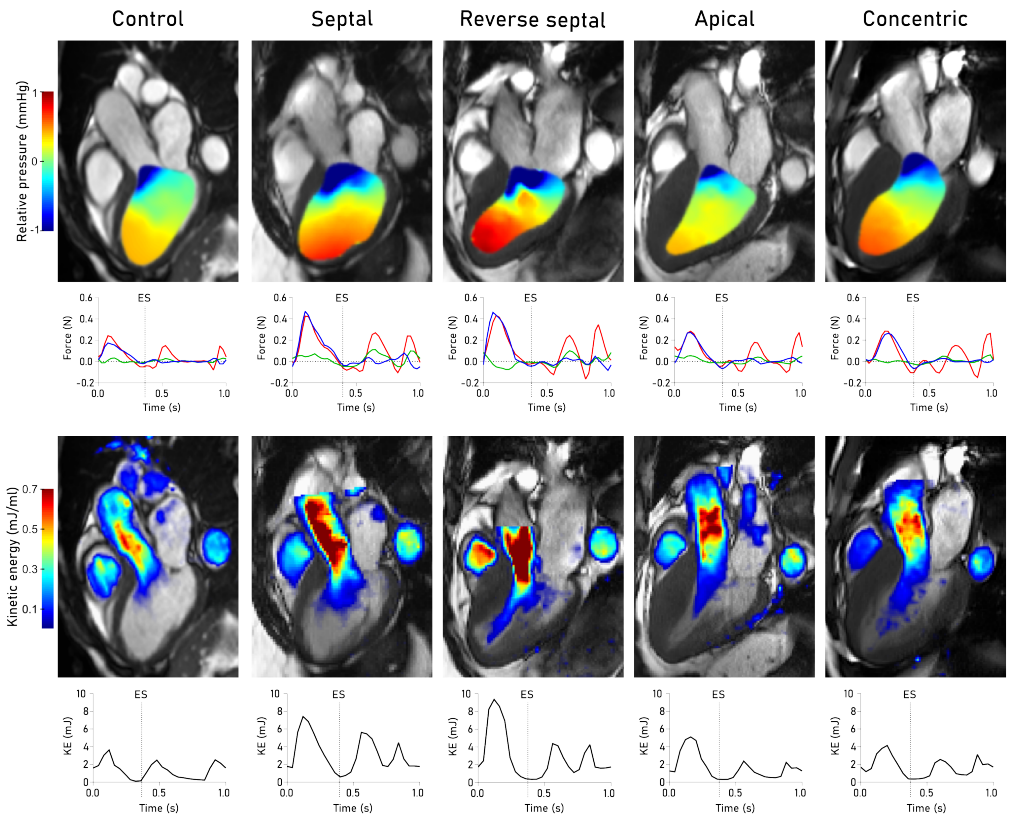

Figure 4.9: Visualization of left ventricular hemodynamic forces and kinetic energy (KE) in one example of a healthy control, and one patient with septal, reverse septal, apical, or concentric hypertrophy. The colored images show relative pressure fields (top row) and kinetic energy (bottom row) during peak systolic flow. The graphs below each image show data for the entire heartbeat in the same study participant, where end systole is marked with "ES".

Systole

In systole, patients with phenotype positive HCM had higher peak kinetic energy and hemodynamic force ratio compared to controls (Figure 4.10). When analyzing subgroups with different patterns of hypertrophy, patients with septal and reverse septal hypertrophy had higher peak systolic kinetic energy compared to controls. Furthermore, patients with apical hypertrophy had higher force ratio compared to controls.

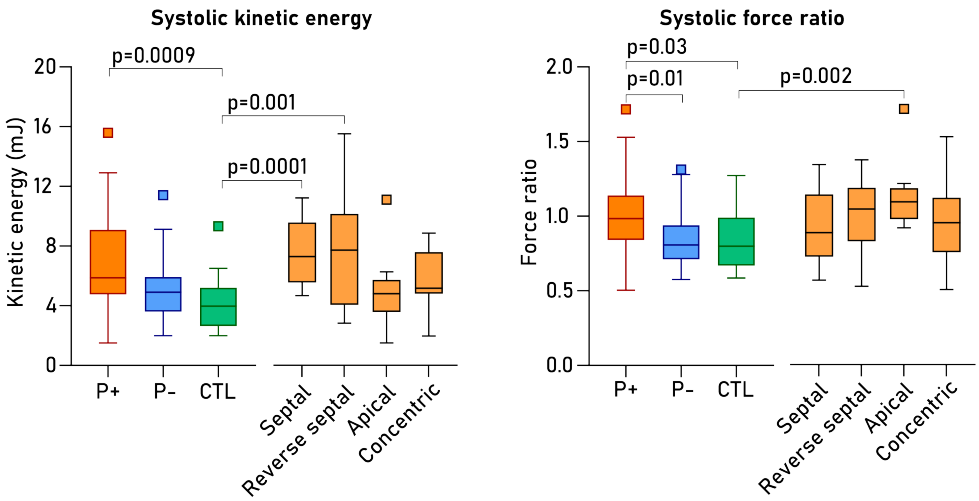

Figure 4.10: Systolic peak kinetic energy and hemodynamic force ratio in patients with hypertrophic cardiomyopathy, categorized as phenotype positive (P+) or negative (P-). The phenotype positive patients were further analyzed based on the pattern of ventricular remodeling, categorized as septal, reverse septal, apical, or concentric hypertrophy. A group of controls (CTL) was included for comparison.

Visual interpretation of the 4D-flow data indicate that higher kinetic energy in patients is influenced by the extent of the constriction of the left ventricular outflow tract. Although all patients were categorized as non-obstructive, the hypertrophied left ventricle in many cases presented with a narrow outflow tract with high blood-flow velocities, especially in patients with septal and reverse septal hypertrophy. Moreover, the maximum wall thickness was positively associated with increased systolic kinetic energy and hemodynamic force ratio in phenotype positive patients (KE: $r = 0.5$, $p < 0.0001$, HDF ratio: $r = 0.3$, $p = 0.004$).

Since hemodynamic force ratio is measured as transverse/longitudinal forces, a higher force ratio means a larger proportion of transverse forces in relation to lon-

gitudinal forces. In patients with apical hypertrophy, a higher force ratio is likely due to a smaller and more spherical left ventricle, resulting in a shorter relative distance of the blood flow in the longitudinal direction. Another plausible explanation is increased transverse contribution to ventricular pumping due to a disorganized micro-anatomy and impaired function on the cellular level, which can be seen in HCM and contribute to dysfunctional contraction.

Diastole

In *early* diastole, patients with HCM but with a normal ventricular anatomy, so called genotype positive and phenotype negative (P-), had higher kinetic energy compared to phenotype positive patients (P+) (Figure 4.11). In the healthy heart, early diastolic blood flow constitutes the major part of ventricular filling (127; 5). However, the proportion of early filling tends to decrease with age as the ventricle may become more stiff. In this study, P- patients were younger than P+ patients and controls, which could be a contributing factor to higher early diastolic kinetic energy P-, in line with previous studies (128; 129).

In *late* diastole, P+ patients had higher peak kinetic energy compared to P- patients and controls (Figure 4.11). Subgroup analysis based on the pattern of hypertrophy showed that mainly patients with septal and reverse septal hypertrophy had higher kinetic energy compared to controls. Late diastolic kinetic energy primarily reflects the filling of the ventricle due to atrial contraction. Therefore, the results in late diastole imply increased atrial contribution to ventricular filling in P+ patients compared to P- and controls, which may be due to a more stiff ventricle in P+ with a larger extent of hypertrophy.

Hemodynamic forces were measured as average values over the entire diastolic phase of the heartbeat, and *not* as early and late diastolic values. This analysis method was chosen after visual interpretation of the time-resolved hemodynamic force data, where there were no clear peaks in one or more directions in the majority of patients. Diastolic force ratio was *lower* in P- patients compared to controls (Figure 4.11), which indicates a *higher* proportion of longitudinal forces in relation to the transverse components, likely reflecting better ventricular relaxation in P- compared to the older controls. Similar to the results in systole, patients with apical hypertrophy also had higher force ratio in diastole compared to controls, which may be due to the smaller and more spherical left ventricle in this group of patients.

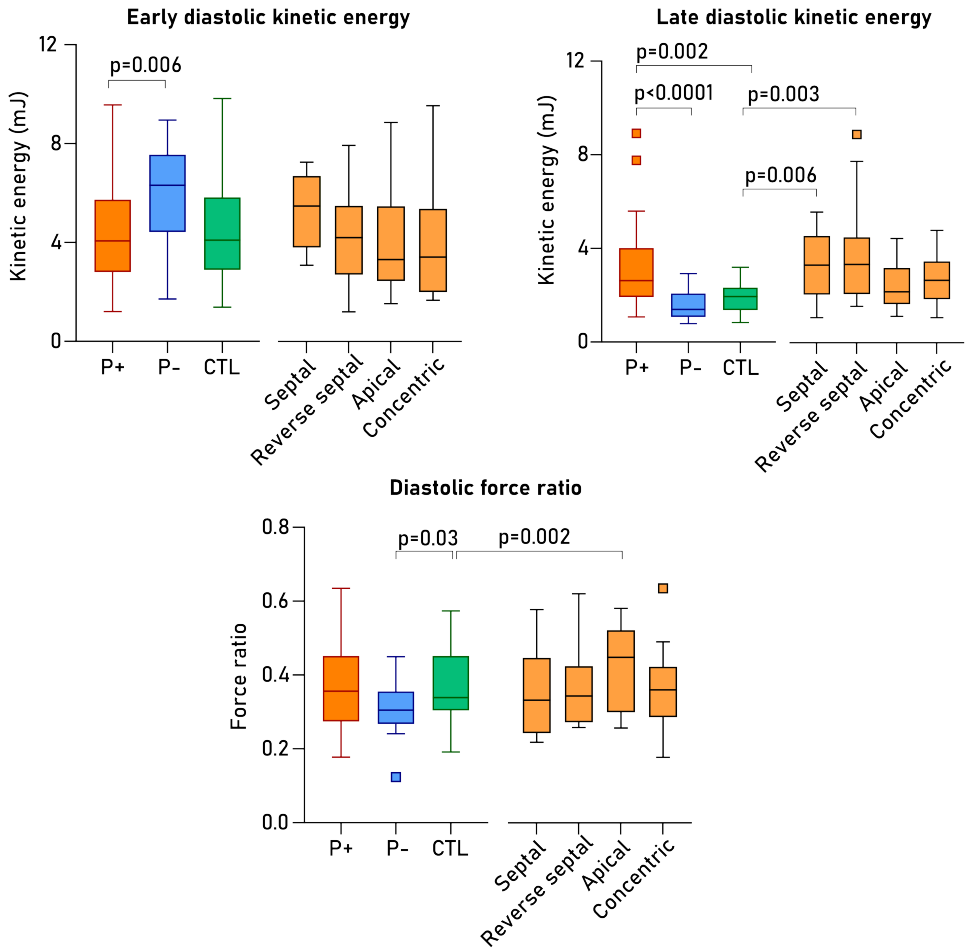

Figure 4.11: Early and late diastolic peak kinetic energy, and diastolic hemodynamic force ratio in patients with hypertrophic cardiomyopathy, categorized as phenotype positive (P+) or negative (P-). The phenotype positive patients were further analyzed based on the pattern of ventricular remodeling, categorized as septal, reverse septal, apical, or concentric hypertrophy. A group of controls (CTL) was included for comparison.

4.4 Study IV

The results in Study IV indicate that clinical evaluation of patients with heart failure and left bundle branch block may be improved using 4D-flow data from cardiovascular magnetic resonance imaging. The data show that hemodynamic-force analysis from 4D flow before pacemaker implantation, has potential to identify some patients who are unlikely to respond to cardiac resynchronization therapy, despite fulfilling current clinical selection criteria.

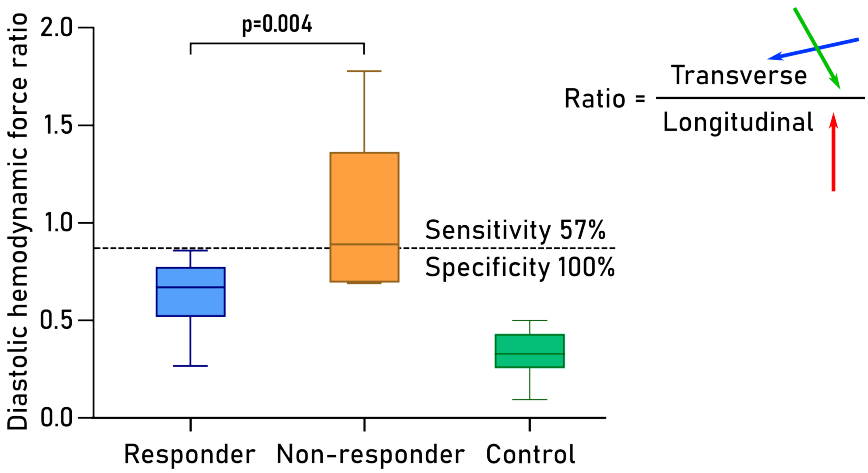

Figure 4.12: Hemodynamic force ratio in diastole in responders and non-responders to cardiac resynchronization therapy, and in controls matched to patients for age and sex. A specificity of 100% for non-response, resulted in a cut-off ratio of >0.87 for non-responders, with a sensitivity of 57%.

Non-responders to CRT had a higher diastolic force ratio compared to responders, as measured before pacemaker implantation (Figure 4.12). A higher force ratio means a larger proportion of transverse forces in relation to the longitudinal component, and may be a sign of dyssynchronous ventricular contraction and relaxation, in keeping with previous studies (92; 94). A receiver operating characteristics (ROC) analysis of diastolic force ratio as a binary classifier of response to CRT, resulted in and area under the curve of 0.88 (Figure 4.13). Identification of non-responders with a specificity of 100% resulted in a cut-off ratio of >0.87 in diastolic force ratio for non-responders, with a sensitivity of 57%. Thus, the results in Study IV indicate that about half of the patients who are unlikely to respond to CRT may be identified by analyzing hemodynamic forces from 4D-flow CMR in addition to standard clinical evaluation before pacemaker implantation.

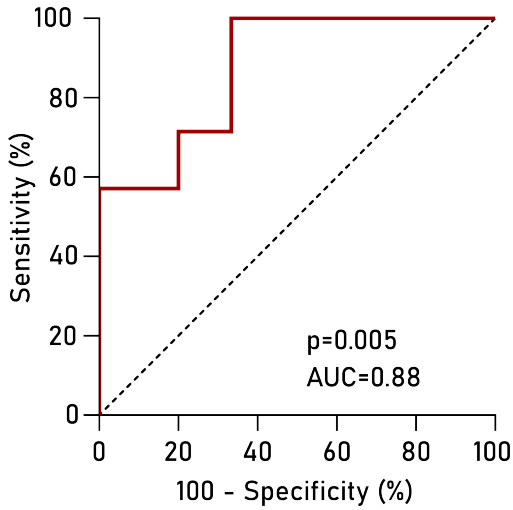

Figure 4.13: A receiver operating characteristic curve for diastolic force ratio as a binary classifier of response to cardiac resynchronization therapy, with an area under the curve (AUC) of 0.88. Dashed line of equality.

Furthermore, when comparing changes in hemodynamic force ratio from systole to diastole, non-responders presented different results compared to responders and controls (Figure 4.14). While both responders and controls exhibited changes with smaller force ratio in diastole compared to systole, no change was seen in non-responders at the group level. In other words, responders exhibited 4D-flow patterns similar to that seen in controls, while non-responders deviated.

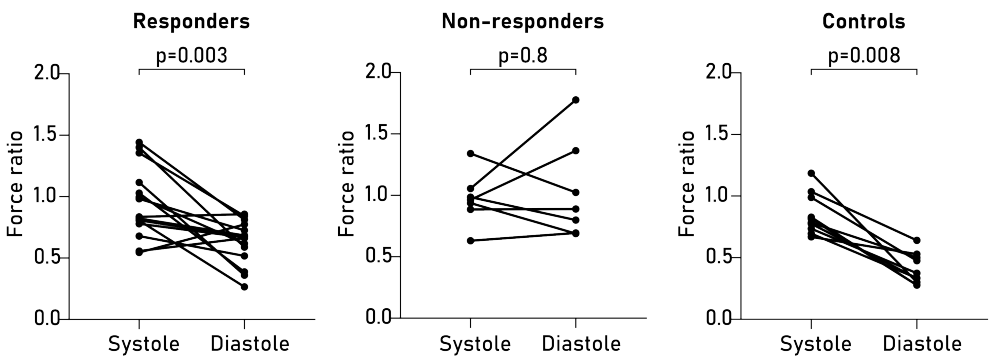

Figure 4.14: Comparisons of the change in hemodynamic force ratio from systole to diastole within the groups of responders and non-responders to cardiac resynchronization therapy, and in controls.

Notably, current clinical selection criteria for CRT are primarily based on evaluation of *systolic* function with ECG and echocardiography, while the results in Study IV show aberrant *diastolic* 4D-flow patterns. Thus, patients who do not respond to CRT may suffer from diastolic dysfunction where CRT does not provide sufficient support.

Chapter 5

Discussion and limitations

In this thesis, heart function was studied using magnetic resonance imaging for analysis of pressure-volume loops of the left ventricle, and blood-flow patterns within the left and right ventricles, in patients at risk for, or with established heart failure with various phenotypes. The four studies demonstrate that novel markers of heart function can contribute to a more nuanced understanding of pathological mechanisms in patients with heart failure, and have potential to provide clinically useful information. Still, each method carries limitations that should be taken into consideration in the interpretation of the results.

In Study I, load alteration was evaluated on non-invasive pressure-volume loops using infusion of saline or glyceryl trinitrate to manipulate preload and afterload. Left ventricular volumes can be measured accurately and precisely with CMR, but the short-axis cine bSSFP images represent a mean heartbeat and may therefore disguise volumetric variations during load manipulation. Moreover, measurements of contractility on non-invasive pressure-volume loops depend on the the position of the x-axis intercept (V_0), which was estimated to $V_0 = 0$ in the research projects in this thesis. In reality, V_0 is subject specific (130), and is likely affected by ventricular pathology such as increased stiffness in hypertrophic cardiomyopathy. Interpretations of contractility measured from non-invasive pressure-volume loops therefore comes with limitations in patients with different phenotypes of heart failure (131). To further improve the analysis of contractility, serial measurements of dynamic, non-invasive pressure-volume loops could be of interest, for example in an experimental model where load may be manipulated with minimal impact on the left ventricular end-systolic pressure-volume slope.

In studies II, III and IV, hemodynamic forces were computed from intraventricular pressure gradients measured with CMR and 4D-flow analysis (132; 133). Hemodynamic forces can also be computed using other methods, such as echocardiography where measurements of intraventricular pressure gradients have been demonstrated in animal experiments (6) and in human (134; 97). Hemodynamic forces can also be estimated from CMR cine bSSFP images and measurements of endocardial borders of the left ventricle (135). When comparing the methods, echocardiography is generally more accessible than CMR, and the temporal resolution is higher with echocardiography. On the other hand, echocardiographic assessment of hemodynamic forces requires contrast infusion with microbubbles, which is not needed with CMR. All three methods provide similar patterns of longitudinal forces, but transverse forces are primarily captured with 4D flow CMR (135).

In Study III, patients with HCM were examined with echocardiography both at rest and during Valsalva maneuver, but the CMR 4D-flow data was acquired only at rest due to the acquisition time of around five to ten minutes for the 4D-flow data. The Valsalva maneuver is a breathing technique where the patient exhales forcefully against a closed airway, which leads to an increased pressure within the chest. The increased pressure results in a reduced venous return to the heart, and consequently a decrease in blood pressure and a compensatory increase in heart rate. In patients with HCM, the Valsalva maneuver can reveal left ventricular outflow tract obstruction as the preload decreases and the left ventricular cavity becomes smaller and presents with a more narrow outflow tract. Thus, blood-flow assessment with echocardiography during Valsalva maneuver may register peak velocities within the left ventricle that cannot be evaluated with a CMR examination and 4D-flow data acquisition at rest.

Study IV investigated the value of hemodynamic-force analysis for prediction of CRT response. Previous studies have demonstrated several parameters associated with a favorable outcome after CRT, such as QRS duration >150 ms and non-ischemic cardiomyopathy (61), as well as myocardial work and septal scar measured using CMR (136; 137). These parameters should therefore be kept in mind when interpreting the results in Study IV, where the study population was too small to allow for any adjustments of confounders in the data analysis. In particular, the proportion of ischemic heart disease was higher in non-responders compared to responders in Study IV. Moreover, patients with atrial fibrillation were not included in Study IV due to technical limitations of 4D-flow data acquisition with CMR.

The prevalence of atrial fibrillation is about 30% in patients receiving CRT, and is associated with a worse prognosis compared to patients with sinus rhythm at baseline (138), which limits the generalization of the results in Study IV.

Since the patient inclusion in Study IV, which took place in the years 2011-2014, left bundle branch area pacing (LBBAB) has emerged as an alternative to the traditional biventricular pacemaker in CRT. The idea behind LBBAP is to obtain a more physiological pacing by stimulating the left bundle branch area. When successful, LBBAP results in more narrow QRS-complexes compared to a biventricular pacemaker, but the implantation procedure can be more technically demanding as LBBAP requires precise targeting of the left bundle branch area. Recent studies indicate that LBBAP leads to lower risks of morbidity and improved heart function compared to a biventricular pacemaker in CRT (139; 140), but the long-term outcomes after LBBAP and the patient selection criteria are domains where more research is still warranted.

Chapter 6

Conclusions and future directions

The overall conclusion of this thesis is that in patients at risk for or with established heart failure, novel biomarkers on cardiovascular magnetic resonance imaging provide new insights in pathological mechanisms of the left and right ventricle. These imaging markers can identify and quantify specific patterns of blood flow and mechanistic properties, and may carry valuable clinical information complementary to standard heart-failure classification. Specific conclusions for each study and future directions are discussed below.

Study I

Non-invasive pressure-volume analysis from CMR can detect cardiac response to altered preload and afterload in healthy participants and in patients with abnormal ventricular filling, in this study patients with HCM. This method and has the potential to provide incremental information to more established measures of cardiac function in clinical practice.

To further study the clinical relevance of non-invasive pressure-volume analysis, longitudinal assessment of patients with heart failure could be of interest. Can non-invasive pressure-volume loops be valuable when evaluating treatment response in patients with heart failure? Previous studies have demonstrated a potential application of non-invasive pressure-volume loops for risk stratification of patients with heart failure or myocardial infarction (141; 142; 143). However, many patients with heart failure or myocardial infarction also exhibit aortic stenosis or mitral in-

sufficiency (144; 145; 146; 147), and the performance of non-invasive pressure-volume loop analysis has not been evaluated in these conditions. Future studies could therefore include patients with various pressure anomalies, who would be assessed with non-invasive pressure-volume loops as well as with invasive measurements for comparison. As pressure disturbances can affect both the left and right side of the heart, developing non-invasive methods for right ventricular pressure-volume loops could also be an interesting research area, with potential applications in patients with pulmonary hypertension.

Study II

In patients with precapillary pulmonary hypertension, 4D-flow CMR with analysis of hemodynamic forces conveys new information of right and left ventricular pumping mechanisms.

To assess the clinical value of 4D-flow data in patients with precapillary pulmonary hypertension, future studies could evaluate 4D-flow measures as markers of heart function in longitudinal studies, and examine relations to invasive pressure measurements performed routinely in clinical practice. Can CMR with 4D flow reduce the need for repeated invasive measurements of pressure and resistance?

Moreover, there is limited research on the overall biological variability of 4D-flow parameters. When studying patients and comparing to controls, patients and controls should be matched regarding variables that could influence the results. How is hemodynamic-force analysis affected by biological parameters such as age, sex, fluid status, and sympathetic activity? Does heart rate affect hemodynamic forces?

Study III

Despite normal blood-flow measurements on echocardiography, patients with non-obstructive hypertrophic cardiomyopathy exhibit abnormal left ventricular blood-flow patterns on 4D-flow CMR. These novel markers of cardiac function carry potential as diagnostics instruments complementary to more established tools for guidance in clinical surveillance and monitoring of treatment.

In the early stages of hypertrophic cardiomyopathy, clinical evaluation of patients can be challenging regarding prognosis and risk stratification, as patients can go for many years without any specific symptoms and with normal left ventricular blood flow and pressure gradients measured with echocardiography. Novel markers on

heart function are therefore desirable to enable a more granular assessment of this patient cohort. Longitudinal studies with 4D-flow parameters for risk stratification and outcome prediction could be of interest in the future.

Furthermore, evaluation of patients with 4D-flow CMR during exercise could be of value, when the technical methods allow. Exercise provocation of symptoms and heart dysfunction has been shown clinically valuable in patients with HCM who present with a non-obstructive profile at rest (148; 149). Some patients are asymptomatic at rest but exhibit physical limitations during exercise. such as fatigue, shortness of breath or dizziness. Another option for provocation could be pharmacological stress with dobutamine, which has been shown feasible during examination with 4D-flow CMR (150). However, dobutamine stress has limited specificity for identification of stress-induced obstruction (151).

Study IV

Patients with heart failure and left bundle branch block may benefit from 4D-flow CMR, where hemodynamic-force analysis have the potential to identify patients who are unlikely to respond to cardiac resynchronization therapy.

Since the term ”response” can be described by several definitions which may result in different interpretations of the outcome of patients (152; 153), future studies with larger patient cohorts could be of interest to evaluate 4D flow in relation to a wider range of outcome measures. Response to CRT is a continuous spectrum including combinations of qualitative and hard parameters, such as exercise capacity, quality of life, morbidity and mortality. Larger studies could contribute to a more nuanced assessment of patient outcome and diagnostic measures associated with a beneficial prognosis for the individual patient.

Furthermore, patients with arrhythmia is a non-negligible group among patients considered for CRT, especially atrial fibrillation (154). Patients with atrial fibrillation were not included in Study IV, since current 4D-flow sequences do not provide sufficient data quality during atrial fibrillation (155). More research on 4D flow and arrhythmia would therefore be of interest, both regarding technical development of sequences suited for atrial fibrillation, but also on physiological interpretation of the acquired data during atrial fibrillation. How can systolic and diastolic 4D-flow data be evaluated and interpreted in patients with atrial fibrillation?

Bibliography

[1] Gerber Y, Weston SA, Redfield MM, Chamberlain AM, Manemann SM, Jiang R, et al. A contemporary appraisal of the heart failure epidemic in Olmsted County, Minnesota, 2000 to 2010. JAMA Internal Medicine. 2015 6;175(6):996-1004.

[2] McDonagh TA, Metra M, Adamo M, Gardner RS, Baumbach A, Böhm M, et al. 2021 ESC Guidelines for the diagnosis and treatment of acute and chronic heart failure. European Heart Journal. 2021;42(36):3599-726.

[3] American Heart Association. The Criteria Committee of the New York Heart Association. Nomenclature and Criteria for Diagnosis for Diseases of the Heart and Great Vessels. 9th ed. Boston, Massachusetts: Little Brown & Co; 1994.

[4] Wiggers C. Modern Aspects of the Circulation in Health and Disease. Philadelphia, PA: Lea & Febiger; 1915.

[5] Brecher GA. Experimental Evidence of Ventricular Diastolic Suction. Circulation Research. 1956;IV.

[6] Courtois M, Kovacs Jr SJ, Ludbrook PA. Transmitral Pressure-Flow Velocity Relation Importance of Regional Pressure Gradients in the Left Ventricle During Diastole. Circulation. 1988;78:661-71.

[7] Shmuylovich L, Chung CS, Kovács SJ. Point: Counterpoint: Left ventricular volume during diastasis is/is not the physiological in vivo equilibrium volume and is/is not related to diastolic suction. Journal of Applied Physiology. 2010 8;109(2):606-8.

[8] Chung CS, Karamanoglu M, Kovács SJ. Duration of diastole and its phases as a function of heart rate during supine bicycle exercise. American Journal

of Physiology - Heart and Circulatory Physiology. 2004;287(5 56-5):2003-8.

[9] Frank O. Die Grundform des Arteriellan Pulses. Z Biol. 1899;37:483-526.

[10] Suga H. Analysis of left ventricular pumping by its pressure-volume coefficient. . Journal of Medical Electronics and Biological Engineering. 1969;7(406).

[11] Monroe G, French GX. Left Ventricular Pressure-Volume Relationships and Myocardial Oxygen Consumption in the Isolated Heart. Circulation Research. 1961;IX.

[12] Suga H. Total mechanical energy of a ventricle model and cardiac oxygen consumption. American Journal of Physiology - Heart and Circulatory Physiology. 1979.

[13] Suga H, Sagawa K, Shoukat AA. Load Independence of the Instantaneous Pressure-Volume Ratio of the Canine Left Ventricle and Effects of Epinephrine and Heart Rate on the Ratio. Circulation Research. 1973 3;32.

[14] Seemann F, Arvidsson P, Nordlund D, Kopic S, Carlsson M, Arheden H, et al. Noninvasive Quantification of Pressure-Volume Loops From Brachial Pressure and Cardiovascular Magnetic Resonance. Circulation Cardiovascular imaging. 2019;12(1):e008493.

[15] Seemann F, Heiberg E, Bruce CG, Khan JM, Potersnak A, Ramasawmy R, et al. Non-invasive pressure–volume loops using the elastance model and CMR: a porcine validation at transient pre-loads. European Heart Journal - Imaging Methods and Practice. 2024 1;2(1).

[16] Arvidsson PM, Green PG, Watson WD, Shanmuganathan M, Heiberg E, De Maria GL, et al. Non-invasive left ventricular pressure-volume loops from cardiovascular magnetic resonance imaging and brachial blood pressure: validation using pressure catheter measurements. European Heart Journal - Imaging Methods and Practice. 2023;1(2):1-10.

[17] Sjöberg P, Seemann F, Arheden H, Heiberg E. Non-invasive quantification of pressure-volume loops from cardiovascular magnetic resonance at rest and during dobutamine stress. Clinical Physiology and Functional Imaging. 2021;41(5):467-70.

[18] Sjöberg P, Arheden H, Heiberg E, Stephensen S, Carlsson M. Haemodynamic left-ventricular changes during dobutamine stress in patients with atrial septal defect assessed with magnetic resonance imaging-based pressure–volume loops. Clinical Physiology and Functional Imaging. 2022 11;42(6):422-9.

[19] Berg J, Jablonowski R, Nordlund D, Ryd D, Heiberg E, Carlsson M, et al. Mild hypothermia attenuates ischaemia/reperfusion injury: insights from serial non-invasive pressure-volume loops. Cardiovascular Research. 2023;119(12):2230-43.

[20] Sjöberg P, Clausen H, Arheden H, Liuba P, Hedström E. Atrial septal defect closure in children at young age is beneficial for left ventricular function. European Heart Journal - Imaging Methods and Practice. 2024 1;2(1).

[21] Watson WD, Green PG, Lewis AJM, Arvidsson P, De Maria GL, Arheden H, et al. Retained Metabolic Flexibility of the Failing Human Heart. Circulation. 2023:109-23.

[22] McMurray JJV, Packer M, Desai AS, Gong J, Lefkowitz MP, Rizkala AR, et al. Angiotensin–Neprilysin Inhibition versus Enalapril in Heart Failure. New England Journal of Medicine. 2014 9;371(11):993-1004.

[23] von Romberg E. Über Sklerose der Lungenarterie. Deutsches Archiv für klinische Medizin. 1891;48:197-206.

[24] Humbert M, Kovacs G, Hoeper MM, Badagliacca R, Berger RMF, Brida M, et al. 2022 ESC/ERS Guidelines for the diagnosis and treatment of pulmonary hypertension: Developed by the task force for the diagnosis and treatment of pulmonary hypertension of the European Society of Cardiology (ESC) and the European Respiratory Society (ERS). European Heart Journal. 2022:ehac237.

[25] Hoeper MM, Humbert M, Souza R, Idrees M, Kawut SM, Sliwa-Hahnle K, et al.. A global view of pulmonary hypertension. Lancet Publishing Group; 2016.

[26] Leber L, Beaudet A, Muller A. Epidemiology of pulmonary arterial hypertension and chronic thromboembolic pulmonary hypertension: identification of the most accurate estimates from a systematic literature review. Pulmonary Circulation. 2021;11(1):1-12.

[27] Zelt JGE, Sugarman J, Weatherald J, Partridge ACR, Liang J, Swiston J, et al. Mortality trends in pulmonary arterial hypertension in Canada: a temporal analysis of survival per ESC/ERS guideline era. European Respiratory Journal. 2022 6;59(6).

[28] Kjellström B, Bouzina H, Björklund E, Beaudet A, Edwards SC, Hesselstrand R, et al. Five year risk assessment and treatment patterns in patients with chronic thromboembolic pulmonary hypertension. ESC Heart Failure. 2022 10;9(5):3264-74.

[29] Rich S. Primary Pulmonary Hypertension. Progress in Cardiovascular Diseases. 1988 11;31(3):205-38.

[30] Hanson J, Huxley H. Structural basis of the cross-striations in muscle. Nature. 1953;172:530-2.

[31] Huxley AF, Niedergerke DR. Structural changes in muscle during contraction - Interference Microscopy of Living Muscle Fibres. Nature. 1954;173:971973.

[32] Maron BJ, Gardin JM, Flack JM, Gidding SS, Kurosaki TT, Bild DE. Prevalence of Hypertrophic Cardiomyopathy in a General Population of Young Adults. Circulation. 1995 8;92(4):785-9.

[33] Teare D. Asymmetrical hypertrohpy of the heart in young adults. British Heart Journal. 1958;20:1-8.

[34] Braunwald E, Lambrew C, Rockoff D, Ross J, Morrow A. Idiopathic Hypertrophic Subaortic Stenosis: I. A Description of the Disease Based Upon an Analysis of 64 Patients. Circulation. 1964 11;29(5s4).

[35] Davies MJ, McKenna WJ. Hypertrophic cardiomyopathy — pathology and pathogenesis. Histopathology. 1995;26(6):493-500.

[36] Sutton M, Tajik AJ, Gibson DG, Brown DJ, Seward JB, Giuliani ER. Echocardiographic Assessment of Left Ventricular Filling and Septal and Posterior Wall Dynamics in Idiopathic Hypertrophic Subaortic Stenosis. Circulation. 1978;57:512-20.

[37] Sanderson JE, Traill TA, St John Sutton MG, Brown DJ, Gibson DG, Goodwin JF. Left ventricular relaxation and filling in hypertrophic cardiomyopathy An echocardiographic study. British Heart journal. 1978;40:596-601.

[38] Cannon R, Rosing DR, Maron BJ, Leon MB, Bonow R, Watson RM, et al. Myocardial ischemia in patients with hypertrophic cardiomyopathy: contribution of inadequate vasodilator reserve and elevated left ventricular filling pressures. Circulation. 1985;71(2):234-43.

[39] Maron BJ, Wolfson JK, Epstein SE, Roberts WC. Intramural ("small vessel") coronary artery disease in hypertrophic cardiomyopathy. Journal of the American College of Cardiology. 1986 9;8(3):545-57.

[40] Dass S, Cochlin LE, Suttie JJ, Holloway CJ, Rider OJ, Carden L, et al. Exacerbation of cardiac energetic impairment during exercise in hypertrophic cardiomyopathy: A potential mechanism for diastolic dysfunction. European Heart Journal. 2015;36(24):1547-54.

[41] Ommen SR, Ho CY, Asif IM, Balaji S, Burke MA, Day SM, et al.. 2024 AHA/ACC/AMSSM/HRS/PACES/SCMR Guideline for the Management of Hypertrophic Cardiomyopathy: A Report of the American Heart Association/American College of Cardiology Joint Committee on Clinical Practice Guidelines. Lippincott Williams and Wilkins; 2024.

[42] Richard P, Charron P, Carrier L, Ledeuil C, Cheav T, Pichereau C, et al. Hypertrophic cardiomyopathy: Distribution of disease genes, spectrum of mutations, and implications for a molecular diagnosis strategy. Circulation. 2003 5;107(17):2227-32.

[43] Ho CY, Day SM, Ashley EA, Michels M, Pereira AC, Jacoby D, et al. Genotype and lifetime burden of disease in hypertrophic cardiomyopathy insights from the sarcomeric human cardiomyopathy registry (SHaRe). Circulation. 2018;138(14):1387-98.

[44] Rickers C, Wilke NM, Jerosch-Herold M, Casey SA, Panse P, Panse N, et al. Utility of cardiac magnetic resonance imaging in the diagnosis of hypertrophic cardiomyopathy. Circulation. 2005 8;112(6):855-61.

[45] Noureldin RA, Liu S, Nacif MS, Judge DP, Halushka MK, Abraham TP, et al.. The diagnosis of hypertrophic cardiomyopathy by cardiovascular magnetic resonance; 2012.

[46] Nagueh SF, Phelan D, Abraham T, Armour A, Desai MY, Dragulescu A, et al. Recommendations for Multimodality Cardiovascular Imaging of Patients with Hypertrophic Cardiomyopathy: An Update from the American

Society of Echocardiography, in Collaboration with the American Society of Nuclear Cardiology, the Society for Cardiovascular Magnetic Resonance, and the Society of Cardiovascular Computed Tomography. Journal of the American Society of Echocardiography. 2022 6;35(6):533-69.

[47] Maron MS, Olivotto I, Zenovich AG, Link MS, Pandian NG, Kuvin JT, et al. Hypertrophic cardiomyopathy is predominantly a disease of left ventricular outflow tract obstruction. Circulation. 2006 11;114(21):2232-9.

[48] Maron MS, Olivotto I, Betocchi S, Casey SA, Lesser JR, Losi MA, et al. Effect of Left Ventricular Outflow Tract Obstruction on Clinical Outcome in Hypertrophic Cardiomyopathy. New England Journal of Medicine. 2003;348:295-303.

[49] O'Mahony C, Jichi F, Pavlou M, Monserrat L, Anastasakis A, Rapezzi C, et al. A novel clinical risk prediction model for sudden cardiac death in hypertrophic cardiomyopathy (HCM Risk-SCD). European Heart Journal. 2014 8;35(30):2010-20.

[50] Eppinger H, Rothberger C. Zur Analyse des Elektrokardiogramms. Wien Klin Wochenschr. 1909;22:1091-8.

[51] Kligfield P, Gettes LS, Bailey JJ, Childers R, Deal BJ, Hancock EW, et al. Recommendations for the standardization and interpretation of the electrocardiogram: Part I. Circulation. 2007 3;115(10):1306-24.

[52] Eppinger H, Stoerk O. Zur Klinik des Elektrokardiogramms. Klin Med. 1910;71:157-64.

[53] Lewis T. The Spread of the Excitatory Process in the Vertebrate Heart. Philosophical Transactions of the Royal Society of London. 1916;207:221-310.

[54] Barker P, Macleod G, Alexander J. The Excitatory Process Observed In The Exposed Human Heart. American Heart Journal. 1930;5:720-42.

[55] Wilson F, Macleod G, Barker P. Electrocardiographic leads which record potential variations produced by the heart beat at a single point. Proc Soc Exp Biol Med. 1932;29:110-2.

[56] Olson S, Shafer P, Wooley CF. Functional Abnormalities in Isolated Left Bundle Branch Block. Circulation. 1989;79(4):845-53.

[57] Sadaniantz A, Laurent LS. Left Ventricular Doppler Diastolic Filling Patterns in Patients With Isolated Left Bundle Branch Block. American Journal of Cardiology. 1998;81:643-5.

[58] Surawicz B, Childers R, Deal B, Gettes L, Bailey J, Gorgels A, et al. AHA / ACCF / HRS Recommendations for the Standardization and Interpretation of the Electrocardiogram: Part III. JAC. 2009;53(11):976-81.

[59] Baldasseroni S, Opasich C, Gorini M, Lucci D, Marchionni N, Marini M, et al. Left bundle-branch block is associated with increased 1-year sudden and total mortality rate in 5517 outpatients with congestive heart failure: A report from the Italian Network on Congestive Heart Failure. American Heart Journal. 2002;143(3):398-405.

[60] Ehra A, Task A, Members F, Glikson M, Israel C, Denmark C, et al. 2021 ESC Guidelines on cardiac pacing and cardiac resynchronization therapy. 2021:1-94.

[61] Hsu JC, Solomon SD, Bourgoun M, Mcnitt S, Goldenberg I, Klein H, et al. Predictors of Super-Response to Cardiac Resynchronization Therapy and Associated Improvement in Clinical Outcome. Journal of the American College of Cardiology. 2012;59(25):2366-73.

[62] Cleland JG, Abraham WT, Linde C, Gold MR, Young JB, Claude Daubert J, et al. An individual patient meta-analysis of five randomized trials assessing the effects of cardiac resynchronization therapy on morbidity and mortality in patients with symptomatic heart failure. European Heart Journal. 2013;34(46):3547-56.

[63] Varma N, Boehmer J, Bhargava K, Yoo D, Leonelli F, Costanzo M, et al. Evaluation, Management, and Outcomes of Patients Poorly Responsive to Cardiac Resynchronization Device Therapy. Journal of the American College of Cardiology. 2019 11;74(21):2588-603.

[64] Hancock HC, Close H, Mason JM, Murphy JJ, Fuat A, Singh R, et al. High prevalence of undetected heart failure in long-term care residents: Findings from the Heart Failure in Care Homes (HFinCH) study. European Journal of Heart Failure. 2013;15(2):158-65.

[65] Hanson LG. Is quantum mechanics necessary for understanding magnetic resonance? Concepts in Magnetic Resonance Part A. 2008 9;32A(5):329-40.

[66] Lanzer P, Botvinick EH, Schiller NB, Crooks LE, Arakawa M, Kaufman L, et al. Cardiac imaging using gated magnetic resonance. Radiology. 1984 1;150(1):121-7.

[67] Glover GH, Pelc NJ. A rapid-gated cine MRI technique. Magnetic Resonance Annual. 1988:299-333.

[68] Sondergaard L, Stahlberg F, Thomsen JC, Spraggins TA, Gymoese E, Malmcren L, et al. Comparison between retrospective gating and ECG triggering in magnetic resonance velocity mapping. Magneric Resonance Imaging. 1993;11:533-7.

[69] van Dijk P. Direct Cardiac NMR Imaging of Heart Wall and Blood Flow Velocity. Journal of Computer Assisted Tomography. 1984 6;8(3):429-36.

[70] Lenz GW, Haacke EM, White RD. Retrospective cardiac gating: A review of technical aspects and future directions. Magnetic Resonance Imaging. 1989;7:445-55.

[71] Donald W McRobbie MJGMRP Elizabeth A Moore. MRI from Picture to Proton. 3rd ed. Cambridge University Press; 2003.

[72] Schulz-Menger J, Bluemke DA, Bremerich J, Flamm SD, Fogel MA, Friedrich MG, et al. Standardized image interpretation and post-processing in cardiovascular magnetic resonance - 2020 update: Society for Cardiovascular Magnetic Resonance (SCMR): Board of Trustees Task Force on Standardized Post-Processing. Journal of Cardiovascular Magnetic Resonance. 2020 3;22(19):1-22.

[73] Singer JR. Blood Flow Rates by Nuclear Magnetic Resonance Measurements. Science. 1959;130(3389):1652-3.

[74] Moran PR. A flow velocity zeugmatographic interlace for NMR imaging in humans. Magnetic Resonance Imaging. 1982;1(4):197-203.

[75] Nayler GL, Firmin DN, Longmore DB. Blood flow imaging by cine magnetic resonance. Journal of Computer Assisted Tomography. 1986;10(5):715-22.

[76] Stahlberg F, Mogelvang J, Thomsen C, Nordell B, Stubgaard M, Ericsson A, et al. A method for MR quantification of flow velocities in blood and

CSF using interleaved gradient-echo pulse sequences. Magnetic Resonance Imaging. 1989;7:655-67.

[77] Pelc NJ, Bernstein MA, Shimakawa A, Glover GH. Encoding strategies for three-direction phase-contrast MR imaging of flow. Journal of Magnetic Resonance Imaging. 1991 7;1(4):405-13.

[78] Wigström SL L, Wranne B. Temporally Resolved 3D Phase-Contrast Imaging. Magn Reson Med. 1996;36:800-3.

[79] Nordmeyer S, Riesenkampff E, Messroghli D, Kropf S, Nordmeyer J, Berger F, et al. Four-dimensional velocity-encoded magnetic resonance imaging improves blood flow quantification in patients with complex accelerated flow. Journal of Magnetic Resonance Imaging. 2013;37(1):208-16.

[80] Bissell M, Raimondi F, Ait Ali L, Allen BD, Barker AJ, Bolger A, et al. 4D Flow cardiovascular magnetic resonance consensus statement: 2023 update. Journal of Cardiovascular Magnetic Resonance. 2023;25(40):1-24.

[81] Visby L, Møgelvang R, Grund FF, Myhr KA, Hassager C, Vejlstrup N, et al. The Influence of Food Intake and Preload Augmentation on Cardiac Functional Parameters: A Study Using Both Cardiac Magnetic Resonance and Echocardiography. Journal of Clinical Medicine. 2023 11;12(21).

[82] Taraldsen IA, Mogelvang R, Grund FF, Hassager C, Søgaard P, Kristensen CB. Increased preload and echocardiographic assessment of diastolic function. Echocardiography. 2024 9;41(9).

[83] Watson WD, Green PG, Valkovič L, Herring N, Neubauer S, Rider OJ. Myocardial Energy Response to Glyceryl Trinitrate: Physiology Revisited. Frontiers in Physiology. 2021;12.

[84] Borgquist R, Carlsson M, Markstad H, Werther-Evaldsson A, Ostenfeld E, Roijer A, et al. Cardiac Resynchronization Therapy Guided by Echocardiography, MRI, and CT Imaging: A Randomized Controlled Study. JACC: Clinical Electrophysiology. 2020;6(10):1300-9.

[85] Heiberg E, Sjögren J, Ugander M, Carlsson M, Engblom H, Arheden H. Design and validation of Segment-freely available software for cardiovascular image analysis. BMC Medical Imaging. 2010;1(10):1-13. Available from: `http://segment.heiberg.se`.

[86] Tufvesson J, Hedström E, Steding-Ehrenborg K, Carlsson M, Arheden H, Heiberg E. Validation and Development of a New Automatic Algorithm for Time-Resolved Segmentation of the Left Ventricle in Magnetic Resonance Imaging. BioMed Research International. 2015;2015:1-12.

[87] Westerhof N, Stergiopulos N, Noble MIM. Snapshots of Hemodynamics. 2nd ed. Springer; 2004.

[88] Buonocore MH, Bogren H. Factors influencing the accuracy and precision of velocity□encoded phase imaging. Magnetic Resonance in Medicine. 1992 7;26(1):141-54.

[89] Busch J, Giese D, Kozerke S. Image-based background phase error correction in 4D flow MRI revisited. Journal of Magnetic Resonance Imaging. 2017;46(5):1516-25.

[90] Yang GZ, Burger P, Kilner PJ, Karwatowski SP, Firmin DN. Dynamic range extension of cine velocity measurements using motion-registered spatiotemporal phase unwrapping. Journal of Magnetic Resonance Imaging. 1996;6(3):495-502.

[91] Loecher M, Schrauben E, Johnson KM, Wieben O. Phase unwrapping in 4D MR flow with a 4D single-step laplacian algorithm. Journal of Magnetic Resonance Imaging. 2016;43(4):833-42.

[92] Pedrizzetti G, Martiniello AR, Bianchi V, D'Onofrio A, Caso P, Tonti G. Changes in electrical activation modify the orientation of left ventricular flow momentum: Novel observations using echocardiographic particle image velocimetry. European Heart Journal Cardiovascular Imaging. 2016;17(2):203-9.

[93] Sjöberg P, Töger J, Hedström E, Arvidsson P, Heiberg E, Arheden H, et al. Altered biventricular hemodynamic forces in patients with repaired tetralogy of fallot and right ventricular volume overload because of pulmonary regurgitation. American Journal of Physiology - Heart and Circulatory Physiology. 2018;315(6):H1691-702.

[94] Arvidsson PM, Töger J, Pedrizzetti G, Heiberg E, Borgquist R, Carlsson M, et al. Hemodynamic forces using four-dimensional flow MRI: An independent biomarker of cardiac function in heart failure with left ventricular dyssynchrony? American Journal of Physiology - Heart and Circulatory Physiology. 2018;315(6):1627-39.

[95] Lapinskas T, Pedrizzetti G, Stoiber L, Düngen HD, Edelmann F, Pieske B, et al. The Intraventricular Hemodynamic Forces Estimated Using Routine CMR Cine Images: A New Marker of the Failing Heart. JACC: Cardiovascular Imaging. 2019;12(2):377-9.

[96] Arvidsson PM, Nelsson A, Magnusson M, Smith JG, Carlsson M, Arheden H. Hemodynamic force analysis is not ready for clinical trials on HFpEF. Scientific Reports. 2022:1-9.

[97] Pedrizzetti G, Martiniello AR, Bianchi V, D'Onofrio A, Caso P, Tonti G. Cardiac fluid dynamics anticipates heart adaptation. Journal of Biomechanics. 2015;48(2):388-91.

[98] Eriksson J, Bolger AF, Carlhäll CJ, Ebbers T. Spatial heterogeneity of four-dimensional relative pressure fields in the human left ventricle. Magnetic Resonance in Medicine. 2015;74(6):1716-25.

[99] Eriksson J, Bolger AF, Ebbers T, Carlhäll CJ. Assessment of left ventricular hemodynamic forces in healthy subjects and patients with dilated cardiomyopathy using 4D flow MRI. Physiological Reports. 2016;4(3):1-12.

[100] Töger J, Arvidsson PM, Bock J, Kanski M, Pedrizzetti G, Carlsson M, et al. Hemodynamic forces in the left and right ventricles of the human heart using 4D flow magnetic resonance imaging: Phantom validation, reproducibility, sensitivity to respiratory gating and free analysis software. PLoS ONE. 2018;13(4):1-22.

[101] Prec O, Katz LN, Sennett L, Rosenman R, Fishman A, Hwang W. Determination of kinetic energy of the heart in man; 1949.

[102] Stefanadis C, Dernellis J, Lambrou S, Toutouzas P. Left Atrial Energy in Normal Subjects, in Patients With Symptomatic Mitral Stenosis, and in Patients With Advanced Heart Failure. American Journal of Cardiology. 1998;(82):1220-3.

[103] Carlsson M, Heiberg E, Toger J, Arheden H. Quantification of left and right ventricular kinetic energy using four-dimensional intracardiac magnetic resonance imaging flow measurements. American Journal of Physiology - Heart and Circulatory Physiology. 2012;302(4).

[104] Arvidsson PM, Töger J, Heiberg E, Carlsson M, Arheden H. Quantification of left and right atrial kinetic energy using four-dimensional intracardiac magnetic resonance imaging flow measurements. Journal of Applied Physiology. 2013;114(10):1472-81.

[105] Kanski M, Arvidsson PM, Töger J, Borgquist R, Heiberg E, Carlsson M, et al. Left ventricular fluid kinetic energy time curves in heart failure from cardiovascular magnetic resonance 4D flow data. Journal of Cardiovascular Magnetic Resonance. 2015;17(1):1-10.

[106] Steding-Ehrenborg K, Arvidsson PM, Töger J, Rydberg M, Heiberg E, Carlsson M, et al. Determinants of kinetic energy of blood flow in the four-chambered heart in athletes and sedentary controls. American Journal of Physiology - Heart and Circulatory Physiology. 2016;310(1):H113-22.

[107] Bolger AF, Heiberg E, Karlsson M, Wigström L, Engvall J, Sigfridsson A, et al. Transit of blood flow through the human left ventricle mapped by cardiovascular magnetic resonance. Journal of Cardiovascular Magnetic Resonance. 2007 9;9(5):741-7.

[108] Eriksson J, Carlhäll C, Dyverfeldt P, Engvall J, Bolger A, Ebbers T. Semi-automatic quantification of 4D left ventricular blood flow. Journal of Cardiovascular Magnetic Resonance. 2010;12(1).

[109] Eriksson J, Bolger AF, Ebbers T, Carlhäll CJ. Four-dimensional blood flow-specific markers of LV dysfunction in dilated cardiomyopathy. European Heart Journal Cardiovascular Imaging. 2013;14(5):417-24.

[110] Svalbring E, Fredriksson A, Eriksson J, Dyverfeldt P, Ebbers T, Bolger AF, et al. Altered diastolic flow patterns and kinetic energy in subtle left ventricular remodeling and dysfunction detected by 4D flow MRI. PLoS ONE. 2016;11(8):1-12.

[111] Ashkir Z, Johnson S, Lewandowski AJ, Hess A, Wicks E, Mahmod M, et al. Novel insights into diminished cardiac reserve in non-obstructive hypertrophic cardiomyopathy from four-dimensional flow cardiac magnetic resonance component analysis. European Heart Journal - Cardiovascular Imaging. 2023;00:1-9.

[112] Trudnowski RJ, Rico RC. Specific gravity of blood and plasma at 4 and 37 °C. Clinical Chemistry. 1974;20(5):615-6.

[113] Mitchell C, Rahko PS, Blauwet LA, Canaday B, Finstuen JA, Foster MC, et al. Guidelines for Performing a Comprehensive Transthoracic Echocardiographic Examination in Adults: Recommendations from the American Society of Echocardiography. Journal of the American Society of Echocardiography. 2018 1;32(1):1-64.

[114] Freemantle N, Tharmanathan P, Calvert MJ, Abraham WT, Ghosh J, Cleland JGF. Cardiac resynchronisation for patients with heart failure due to left ventricular systolic dysfunction - a systematic review and meta-analysis. European Journal of Heart Failure. 2006;8(4):433-40.

[115] Wells G, Parkash R, Healey JS, Talajic M, Arnold JM, Sullivan S, et al. Cardiac resynchronization therapy: A meta-analysis of randomized controlled trials. Cmaj. 2011;183(4):421-9.

[116] Altman DG, Bland JM. Measurement in Medicine: The Analysis of Method Comparison Studies. The Statistician. 1983;32(3):307-17.

[117] Bland JM, Altman DG. Statistical methods for assessing agreement between two methods of clinical measurement. The Lancet. 1986 2:307-10.

[118] Ostenfeld E, Stephensen SS, Steding-Ehrenborg K, Heiberg E, Arheden H, Rådegran G, et al. Regional contribution to ventricular stroke volume is affected on the left side, but not on the right in patients with pulmonary hypertension. International Journal of Cardiovascular Imaging. 2016;32(8):1243-53.

[119] Lindholm A, Hesselstrand R, Rådegran G, Arheden H, Ostenfeld E. Decreased biventricular longitudinal strain in patients with systemic sclerosis is mainly caused by pulmonary hypertension and not by systemic sclerosis per se. Clinical Physiology and Functional Imaging. 2019;39(3):215-25.

[120] Carlsson M, Ugander M, Mosén H, Buhre T, Arheden H. Atrioventricular plane displacement is the major contributor to left ventricular pumping in healthy adults, athletes, and patients with dilated cardiomyopathy. American Journal of Physiology - Heart and Circulatory Physiology. 2007;292(3):1452-9.

[121] Carlsson M, Ugander M, Heiberg E, Arheden H. The quantitative relationship between longitudinal and radial function in left, right, and total heart pumping in humans. American Journal of Physiology - Heart and Circulatory Physiology. 2007;293(1):636-44.

[122] Arvidsson PM, Töger J, Carlsson M, Steding-Ehrenborg K, Pedrizzetti G, Heiberg E, et al. Left and right ventricular hemodynamic forces in healthy volunteers and elite athletes assessed with 4D flow magnetic resonance imaging. American Journal of Physiology - Heart and Circulatory Physiology. 2016;312(2):314-28.

[123] Gan CTJ, Holverda S, Marcus JT, Paulus WJ, Marques KM, Bronzwaer JGF, et al. Right ventricular diastolic dysfunction and the acute effects of sildenafil in pulmonary hypertension patients. Chest. 2007;132(1):11-7.

[124] Ryan T, Petrovic O, Dillon JC, Feigenbaum H, Conley MJ, Armstrong WF. An echocardiographic index for separation of right ventricular volume and pressure overload. Journal of the American College of Cardiology. 1985;5(4):918-24.

[125] Chiba Y, Iwano H, Tsuneta S, Tsujinaga S, Meyers B, Vlachos P, et al. Determinants of altered left ventricular suction in pre-capillary pulmonary hypertension. European Heart Journal - Cardiovascular Imaging. 2022;00:1-8.

[126] Sjögren H, Kjellström B, Bredfelt A, Steding-Ehrenborg K, Rådegran G, Hesselstrand R, et al. Underfilling decreases left ventricular function in pulmonary arterial hypertension. International Journal of Cardiovascular Imaging. 2021;37(5):1745-55.

[127] Katz L. The role played by the ventricular relaxation process in filling the ventricle. American Journal of Physiology. 1930;95(3):542-53.

[128] Wong J, Chabiniok R, de Vecchi A, Dedieu N, Sammut E, Schaeffter T, et al. Age-related changes in intraventricular kinetic energy: A physiological or pathological adaptation? American Journal of Physiology - Heart and Circulatory Physiology. 2016;310(6):H747-55.

[129] Crandon S, Westenberg JJM, Swoboda PP, Fent GJ, Foley JRJ, Chew PG, et al. Impact of Age and Diastolic Function on Novel, 4D flow CMR Biomarkers of Left Ventricular Blood Flow Kinetic Energy. Scientific Reports. 2018;8(1):1-11.

[130] Sagawa K. Editorial: The End-systolic Pressure-Volume Relation of the Ventricle: Definition, Modifications and Clinical Use. Circulation. 1981;63(6).

[131] Blaudszun G, Morel DR. Relevance of the volume-axis intercept, V0, compared with the slope of end-systolic pressure-volume relationship in response to large variations in inotropy and afterload in rats. Experimental Physiology. 2011;96(11):1179-95.

[132] Ebbers T, Wigström L, Bolger AF, Engvall J, Karlsson M. Estimation of relative cardiovascular pressures using time-resolved three-dimensional phase contrast MRI. Magnetic Resonance in Medicine. 2001;45(5):872-9.

[133] Ebbers T, Wigström L, Bolger AF, Wranne B, Karlsson M. Noninvasive measurement of time-varying three-dimensional relative pressure fields within the human heart. Journal of Biomechanical Engineering. 2002;124(3):288-93.

[134] Cimino S, Pedrizzetti G, Tonti G, Canali E, Petronilli V, De Luca L, et al. In vivo analysis of intraventricular fluid dynamics in healthy hearts. European Journal of Mechanics, B/Fluids. 2012 9;35:40-6.

[135] Pedrizzetti G, Arvidsson PM, Töger J, Borgquist R, Domenichini F, Arheden H, et al. On estimating intraventricular hemodynamic forces from endocardial dynamics: A comparative study with 4D flow MRI. Journal of Biomechanics. 2017;60(2017):203-10.

[136] Bleeker GB, Kaandorp TAM, Lamb HJ, Boersma E, Steendijk P, De Roos A, et al. Effect of posterolateral scar tissue on clinical and echocardiographic improvement after cardiac resynchronization therapy. Circulation. 2006 2;113(7):969-76.

[137] Aalen JM, Donal E, Larsen CK, Duchenne J, Lederlin M, Cvijic M, et al. Imaging predictors of response to cardiac resynchronization therapy: left ventricular work asymmetry by echocardiography and septal viability by cardiac magnetic resonance. European Heart Journal. 2020 10;41(39):3813-23.

[138] Bilchick KC, Kamath S, Dimarco JP, Stukenborg GJ. Bundle-branch block morphology and other predictors of outcome after cardiac resynchronization therapy in medicare patients. Circulation. 2010 11;122(20):2022-30.

[139] Diaz JC, Sauer WH, Duque M, Koplan BA, Braunstein ED, Marín JE, et al. Left Bundle Branch Area Pacing Versus Biventricular Pacing as Initial Strategy for Cardiac Resynchronization. JACC: Clinical Electrophysiology. 2023 8;9(8):1568-81.

[140] Vijayaraman P, Sharma PS, Cano ⊠, Ponnusamy SS, Herweg B, Zanon F, et al. Comparison of Left Bundle Branch Area Pacing and Biventricular Pacing in Candidates for Resynchronization Therapy. Journal of the American College of Cardiology. 2023 7;82(3):228-41.

[141] Arvidsson PM, Berg J, Carlsson M, Arheden H. Noninvasive Pressure-Volume Loops Predict Major Adverse Cardiac Events in Heart Failure With Reduced Ejection Fraction. JACC: Advances. 2024;3(6).

[142] Nordlund D, Lav T, Jablonowski R, Khoshnood A, Ekelund U, Atar D, et al. Contractility, ventriculoarterial coupling, and stroke work after acute myocardial infarction using CMR-derived pressure-volume loop data. Clinical Cardiology. 2024 1;47(1).

[143] Lav T, Engstrøm T, Kyhl K, Nordlund D, Lønborg J, Engblom H, et al. Non-invasive pressure-volume loops provide incremental value to age, sex, and infarct size for predicting adverse cardiac remodelling after ST-elevation myocardial infarction. European Heart Journal - Imaging Methods and Practice. 2025 1;3(1).

[144] Robbins JD, Maniar PB, Cotts W, Parker MA, Bonow RO, Gheorghiade M. Prevalence and severity of mitral regurgitation in chronic systolic heart failure. American Journal of Cardiology. 2003 2;91(3):360-2.

[145] Bartko PE, Heitzinger G, Pavo N, Heitzinger M, Spinka G, Prausmüller S, et al. Burden, treatment use, and outcome of secondary mitral regurgitation across the spectrum of heart failure: observational cohort study. British Medical Journal. 2021 6;373.

[146] Sharma H, Radhakrishnan A, Nightingale P, Brown S, May J, O'Connor K, et al. Mitral Regurgitation Following Acute Myocardial Infarction Treated by Percutaneous Coronary Intervention—Prevalence, Risk factors, and Predictors of Outcome. American Journal of Cardiology. 2021 10;157:22-32.

[147] Sivaraj K, Arora S, Hendrickson M, Slehria T, Chang PP, Weickert T, et al. Epidemiology and Outcomes of Aortic Stenosis in Acute Decompensated Heart Failure: The ARIC Study. Circulation: Heart Failure. 2023 3;16(3):E009653.

[148] Joshi S, Patel UK, Yao SS, Castenada V, Isambert A, Winson G, et al. Standing and exercise Doppler echocardiography in obstructive hypertrophic car-

diomyopathy: The range of gradients with upright activity. Journal of the American Society of Echocardiography. 2011 1;24(1):75-82.

[149] Ayoub C, Geske JB, Larsen CM, Scott CG, Klarich KW, Pellikka PA. Comparison of Valsalva Maneuver, Amyl Nitrite, and Exercise Echocardiography to Demonstrate Latent Left Ventricular Outflow Obstruction in Hypertrophic Cardiomyopathy. American Journal of Cardiology. 2017 12;120(12):2265-71.

[150] Sundin J, Engvall J, Nylander E, Ebbers T, Bolger AF, Carlhäll CJ. Improved Efficiency of Intraventricular Blood Flow Transit Under Cardiac Stress: A 4D Flow Dobutamine CMR Study. Frontiers in Cardiovascular Medicine. 2020 11;7.

[151] Pellikka PA, Oh JK, Bailey KR, Nichols BA, Monahan KH, Tajik AJ. Dynamic Intraventricular Obstruction During Dobutamine Stress Echocardiography A New Observation. Circulation. 1992;86(5).

[152] Fornwalt BK, Sprague WW, Bedell P, Suever JD, Gerritse B, Merlino JD, et al. Agreement is poor among current criteria used to define response to cardiac resynchronization therapy. Circulation. 2010 5;121(18):1985-91.

[153] Petrovic M, Petrovic M, Milasinovic G, Vujisic Tesic B, Trifunovic D, Petrovic O, et al. Gauging the response to cardiac resynchronization therapy: The important interplay between predictor variables and definition of a favorable outcome. Echocardiography. 2017 3;34(3):371-5.

[154] Khan MZ, Patel K, Zarak MS, Gupta A, Hussian I, Patel K, et al. Association between atrial fibrillation and bundle branch block. Journal of Arrhythmia. 2021 8;37(4):949-55.

[155] Spartera M, Pessoa-Amorim G, Stracquadanio A, Von Ende A, Fletcher A, Manley P, et al. Left atrial 4D flow cardiovascular magnetic resonance: a reproducibility study in sinus rhythm and atrial fibrillation. Journal of Cardiovascular Magnetic Resonance. 2021 12;23(1).

Acknowledgements

I would like to sincerely thank everyone who has been part of the journey leading up to this thesis. What a joyride! The help and support given to me during this process are gifts I will treasure for the rest of my life, and I hope to pay it forward someday. While the words here cannot cover everything I would like to say to everyone, I would like to express my special gratitude to some people.

Håkan, for the inspiration to do the right thing. For putting up with my questions, and for challenging me in research and in personal development. Per, for guiding me through white space and skröfs, and for opening doors to new people, places and ideas.

The researchers in the Lund Cardiac MR group, for sparking discussions and for leading by example. Ellen, for inviting me to research that first summer, and for showing how to get things done. Katarina, for being only a phone call away when I need some perspective on research, and life in general. Johannes, for your helpfulness and patience when answering my questions about MR physics, over and over again. Henrik, for your honesty and enthusiasm in everything you do. Erik, for showing that anything is possible if you put your mind to it. Anthony, for the critical, yet kind, discussions, and for reminding how lucky we are to have ended up right here, right now. Barbro, Einar, Shahnaz, Mariam, Petter, Pia, Björn, Alessandro, and Mattias, for fruitful discussions and fellowship.

The PhD students in the Lund Cardiac MR group, for sharing laughter and labors throughout the past years. Anna, the morning walks, evening scans, and everyday tasks are so much fun with you. Elsa, your kindness is an inspiration, and a cup of tea with you always nourishes the mind. Anders, for giving generously of your time, even when you don't have it. Axel, Kristian, Jonathan, Martin, Tania, Theodor, Marjolein, and Julius, for discussions relating to work and life as a PhD student, and for enriching every day.

All my colleagues at the Department of Clinical Physiology in Lund, for your

optimistic attitude to new ideas and for the welcoming environment. Especially Ann-Helen, Annmarie, Johanna, Lotta, Anna and Ashwin, without you there would be no data to address in this thesis. Jane and Karin, for the immense administrative support, and for finding solutions to every problem. The Medviso team, Fanny, Tony, Ingela, and Cecilia, for being happy to help with anything whenever needed.

The Oxford Centre for Clinical Magnetic Resonance Research, for providing the opportunity to visit for a year during my time as a PhD student. Especially, Professor Stefan Neubauer, for leading a prosperous research group, and Associate Professor Betty Raman, for your supervision and encouragement. Zak, Sarah, Aaron, Azlan, and May, for sharing your expertise and spreading joy. St Hilda's College in Oxford with all the students and staff who made the house feel like home. Mirjam and the Arvidsson family, for your warm welcome during my time in Oxford.

All the study participants, for your generous contributions to research. The funding organizations, for believing that this research is worth investing in.

My friends, for providing a safe space for discussions about anything that comes to mind. Especially Daria, Nora, Noemi, Johanna, Anna and Mathilda. The orchestras and ensembles I have been fortunate to be part of over the years, for the music and meetings. What a blast life is with you!

My dear family, mamma, pappa, Martin and Elin, for stimulating curiosity and supporting unconditionally. Emil, for your wholehearted kindness, patience and honesty.

Lund, April 29th 2025

Part II

Research Papers

Author contributions

	Study I	Study II	Study III	Study IV
Study design	2	0	2	1
Ethical application	0	0	0	0
Data aquisition	0	0	0	0
Data analysis	3	3	3	3
Statistical analysis	3	3	3	3
Figures and tables	3	3	3	3
Interpretation of results	3	3	3	3
Preparation of manuscript	3	2	3	3
Revision of manuscript	-	3	3	3
Reply to reviewers	-	2	3	3

Not yet applicable	-
No contribution	0
Limited contribution	1
Moderate contribution	2
Significant contribution	3

Additional projects not included in this thesis:

4D FORCE

The ongoing study 4D FORCE (Four-Dimensional Flow for Outcome pRediction of CRT Effect) is a continuation of Study IV in this thesis. The main purpose of 4D FORCE is to thoroughly investigate whether 4D flow CMR can be beneficial in clinical evaluation and response prediction of patients eligible for cardiac resynchronization therapy. 4D FORCE is a prospective, longitudinal study with a planned inclusion of n=200 patients. Each study participant undergoes two visits, first at baseline before pacemaker implantation, and then a second examination at six to eight months' follow-up. Both study visits entail taking a medical history, questionnaires about life quality, CMR examination, cardiopulmonary exercise test, and echocardiography.

HORMONE

The purpose of the ongoing study HORMONE (Heart functiOn in Relation to sex horMone variatiONs in womEn) is to investigate myocardial perfusion in women in relation to hormone variations. HORMONE is a prospective study with a planned inclusion of n=100 healthy women, both pre- and post-menopausal. All study participants are examined with CMR and analysis of quantitative myocardial perfusion at rest and stress, and blood samples of hormone levels are collected. The results from this study may provide enhanced insights into the physiology of the healthy female heart, which is the foundation for improved understanding of pathology in future studies, and eventually evolvement of better healthcare for patients with pathological myocardial perfusion, such as ischemic heart disease.

	4D FORCE	HORMONE
Study design	3	3
Ethical application	3	3
Data aquisition	3	3
Data analysis	3	3
Statistical analysis	-	-
Figures and tables	-	-
Interpretation of results	-	-
Preparation of manuscript	-	-
Revision of manuscript	-	-
Reply to reviewers	-	-

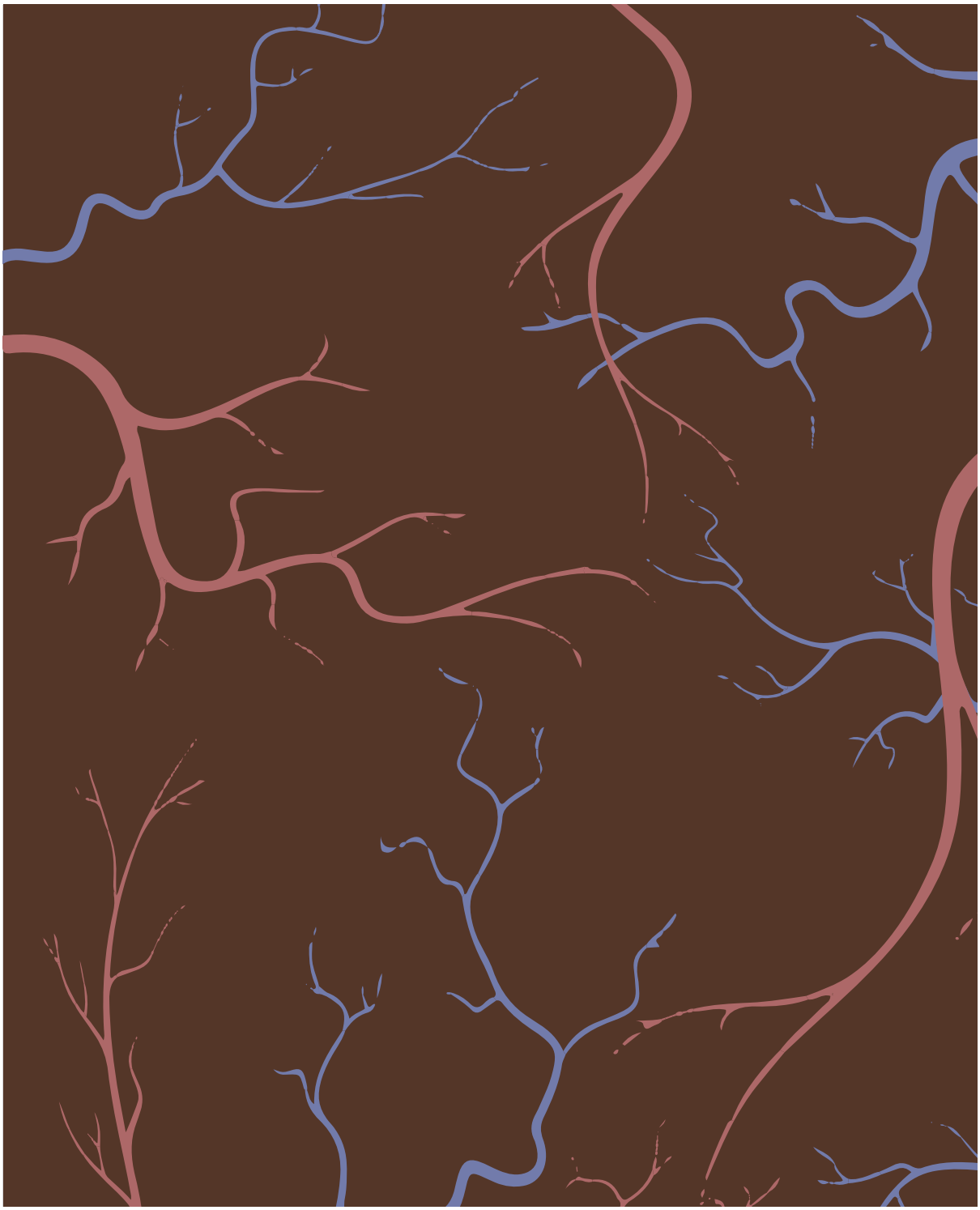

LUND UNIVERSITY

FACULTY OF MEDICINE

Department of Clinical Physiology

Lund University, Faculty of Medicine
Doctoral Dissertation Series 2025:72
ISBN 978-91-8021-725-5
ISSN 1652-8220